Method development for the quantification of rare earth elements in South African monazite by various spectroscopic techniques

UNIVERSITY OF THE
WITWATERSRAND,
JOHANNESBURG

by

Mmantheka Patricia Rangata
2528470

A dissertation submitted to the Faculty of Science, University of the Witwatersrand, Johannesburg in fulfilment of the requirements for the degree of

Master of Science
in
Chemistry

Supervisor: Prof. Luke Chimuka

Co-supervisors: Dr. James Tshilongo

Dr. Andile Mkhohlakali

March 2025

DECLARATION

I declare that this dissertation is my own, unaided work and that it is my work undertaken under the guidance of my supervisors. It is being submitted for the Degree of Master of Science in the University of Witwatersrand, Johannesburg. It has not been submitted before for any degree or examination in any other University.

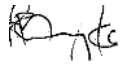

(Signature of candidate)

06 Day of March 2025 at Randburg

ABSTRACT

The rare earth elements are critical, and their various applications include electronics, the defence sector, manufacturing, renewable energy, technology and the medical sciences. The increasing demand for these critical elements will strain the existing supply chain. There is a major concern that any disruption to the supply chain will negatively impact innovation. Countries worldwide are seeking to secure new reserves, find the material substitutes, and boost the research in recycling electronics that have reached the end of life. Monazite contains critical rare-earth-elements responsible for green energy transition.

The bottleneck associated with analysing rare-earth elements in monazite is its refractory nature and associated heavy minerals that do not decompose completely in the sulphuric acid fuming procedure. Furthermore, rare-earth elements have been successfully measured in geological materials employing the sensitive inductively coupled plasma mass spectrometry techniques. Nevertheless, it suffers from a low tolerance of total dissolved solids in matrices such as monazite. While, inductively coupled plasma optical emission spectroscopy suffers from poor sensitivity and matrix removal is often required for accurate rare-earth elements determinations. Extensive research has been conducted on sensitive procedures and efficient sample preparation for trace elements determinations including rare-earth elements.

This study aims to develop a method for direct determination of rare-earth-elements in monazite. The monazite ore samples were collected from the extractive metallurgy within Mintek for method development for quantification of REEs. Three preparation methods for sample digestion techniques were evaluated. The methods involved the flux fusion method using the lithium metaborate and sodium peroxide respectively and the multi acids digestion with hotplate as the source of heat followed by rare earth elements quantification using both the inductively coupled plasma mass

spectrometry and inductively coupled plasma optical emission spectroscopy. Moreover, the complete sample dissolution was achieved with the flux fusion method while the partial sample dissolution was observed via multiple (repetitive) treatment steps by multi acids digestion method. The total dissolved solids were mitigated, and the matrix effect was eliminated when glass beads were treated (dissolved) in a mixture containing nitric and hydrofluoric acids.

The analyte spectrum was often completely obscured by wing overlap and direct overlap of emission lines from interfering elements during-inductively coupled plasma optical emission spectroscopy analysis. In addition, the recoveries for some rare earth elements were suppressed with enhanced spikes for rare earth elements concentration were observed from inductively coupled plasma optical emission analysis particularly from the solution samples digested in alkaline fusion. The inductively coupled plasma optical emission spectroscopy results for the rare earth elements suggest that the sample matrix significantly affects the sensitivity. The method's validity was tested using a monazite ore-certified reference material. In contrast to the optical emission spectroscopy, the accurate analysis of rare earths from all the digested samples was obtained using the inductively coupled plasma mass spectrometry.

The results of the rare earth elements obtained for all digested samples analysed using the mass spectrometry strongly agree with the certified values. The excellent accuracy of the method was realised with the rare earth elements data obtained from quality control samples, and recoveries yield within the range of 90-110%, and the relative standard deviation of 0.2-5.4%. The selectivity and sensitivity of the method were realised with individual rare earths accurately measured in the presence of other interfering elements, as indicated by lower detection of limit ~ (0.0004-0.016 ppm) and limit of quantification ~ (0.0001-0.0290 ppmn). Calibration curve linearity for individual rare earth elements is demonstrated by the correlation

coefficient in the range of 0.99 to 1.0. Moreover, multi fusion methods followed by mass spectrometry are futuristic analytical approaches for determining rare earth elements in monazite associated minerals and they can be used interchangeably. In South African context, South Africa should prioritise the development of Rare Earth Elements (REE) extraction and recycling technologies in order to maximise yield, purity, and environmental sustainability, notably through enhanced procedures for monazite-rich deposits. Investing in a circular economy paradigm, such as boosting REE recovery from electronic trash, can minimise dependency on virgin resources and help to create a more sustainable future. To further help the country's green energy transition, the government should fund research into REE-based technologies critical to renewable energy systems such as wind turbines, solar panels, and electric cars. Furthermore, developing regulatory frameworks that ensure responsible mining techniques and monitor the entire REE supply chain will assist to mitigate environmental and social consequences. Additionally, South Africa can enhance its role in the global REE market by collaborating with international partners, leveraging external expertise, and promoting sustainable technologies, thereby contributing to a low-carbon economy.

DEDICATION

In Memory of My Father (Bra Paul) in
Heaven: **Mr Mashao Abram Rangata** 1948-2015

ACKNOWLEDGEMENTS

My utmost gratitude goes to The Almighty for granting me the opportunity, strength, wisdom and ability to pursue my studies against all odds.

I would like to express my sincere gratitude to my esteemed supervisor, Prof Luke Chimuka, for his unwavering support and guidance throughout this journey.

A very special thanks to Dr. James Tshilongo for going beyond co-supervisor duties through empowering, counselling, and continual support.

Special thanks to my co-supervisor, Dr. Andile Mkhohlakali for his insight and helpful feedback, and for going the extra mile to ensure the study's success.
Special thanks to the Head of Section, Dr. Happy Mabowa for her tremendous contribution to the study.

I acknowledge Mintek for the funding during the Analytical Chemistry Division (ACD) studentship, which allowed me to use the resources and infrastructure for my experimental work in this study. The ACD team thank you for all the assistance and support, especially Dr Moshalagae Motlatle, Mfundo Msimango, Dimakatso Mokgosi, and Mr Napo Ntsasa. The REEs team including Dr Kedibone Mashale, Dr. Odwa Mapazi, Tshilidzi Rampfumedzi, Vhonani Rerani, Xikhongelo Rikhotso, and Mceliseni Zuma for the encouragement and sharing of ideas and insights, thank you.

Lastly, I want like to thank (koko Moloi Mongalo and mma Mmantlatla Selina Rangata) and the entire family for their unwavering support, love and understanding throughout the journey.

PUBLICATIONS AND MANUSCRIPTS

(i) Journals and Publications

M.P Rangata; A. Mkhohlakali; N. Ntsasa; M.H Mabowa; L. Chimuka; and J. Tshilongo. **Title*:*** Hotplate assisted multi acid digestion of monazite for quantification of HREEs using ICP-OES and ICP-MS (2025), (***Under review***)

(ii) Conferences attended

(ii) Oral Presentations: NLA South Africa Test and Measurement Conference 24-26 October 2022, CSIR International Convention Centre. ***Title***: Method development for quantification of rare earth elements (REEs) in monazite samples by various spectroscopic techniques.

(iii) Poster Presentation: Test and Measurement Conference 24-26 October 2024.**Title**: Determination of rare earth elements in monazite using lithium metaborate fusion followed by inductively coupled plasma spectrometry (ICP-MS).

(iv) Conference proceedings

M.P Rangata, A. Mkhohlakali, L. Chimuka, and J. Tshilongo. *Title*: Determination of rare earth elements in monazite using lithium metaborate fusion followed by inductively coupled plasma spectrometry (ICP-MS), Test and Measurement Conference 24-26 October 2024, CSIR International Convention Centre.

Buhle Xakalashe, Elias Matinde, Xolisa Goso, Quinn Reynolds, Lunia Malaka, Vielet Hilane, Thokozile Kekana, Sivanna Hanuman, Ashma Singh, Medhi Safari, Getrude Marape, Taswald Moodley, Walter

Ngobeni, Tsholofelo Koadibane, Tshamano Netshikhudini, Gebhu Ndlovu, Olga Bazhko, Deshenthree Chetty, Yash Thakurdin, Candice Carelse, Refilwe Moeletsi, Beberto Baloyi, Veruska Govender, Jonathan Desebrook, Marian Manuel, Odwa Mapazi, Andile Mkhohlakali, **Patricia Rangata,** Xikhongelo Rikhotso, Happy Mabowa, Vhonani Rerani, Tshilidzi Rampfumedzi, Semakaleng Kganyago, Mceliseni Zuma, Thandukwazi Bungane, Agnes Modiga, Joseph Moema, Maje Phasha, James Tshilongo, Elmar Muller. *Title*: Rare earth elements research conducted at Mintek. Southern African Rare Earths 2nd International Conference 2024, Namibia, 19-20 June 2024 Southern African Institute of Mining and Metallurgy.

TABLE OF CONTENTS

LIST OF FIGURES

LIST OF TABLES

LIST OF ABBREVIATIONS

Al	Aluminium
Ca	Calcium
g	Grams
HREEs	Heavy rare earth elements
Hr	Hour
HCl	Hydrochloric acid
HF	Hydrofluoric acid
ICP-MS	Inductively coupled plasma mass spectrometry
ICP-OES	Inductively coupled plasma optical emission spectroscopy
$LiBO_2$	Lithium metaborate
LREEs	Light rare earth elements
Mg	Magnesium
Mins	Minutes
N.d	Not detected
ppm	Parts per million
%	Percentage
REEs	Rare earth elements
REOs	Rare earth oxides
SARM	South African Reference Material
NaOH	Sodium hydroxides
Na_2O_2	Sodium peroxide
TDS	Total dissolved solids
TREEs	Total rare earth elements
TREO	Total rare earth oxides
Zr	Zirconium

CHAPTER ONE: INTRODUCTION

The dissertation comprises of five chapters. The first chapter outlines the background of the study's aims and objectives, problems statement, the motivation, hypothesis, and research question.

1.1 Background

As defined by the International Union of Pure and Applied Chemistry (IUPAC), rare earth elements (REEs) include fifteen lanthanides on the periodic table and since yttrium and scandium frequently occur in the same ore deposits as the lanthanides, they are considered rare earths. Various applications of rare earth elements (REEs) in green energy technology include the transforming to a low carbon-economy. Green chemistry makes rare earths the most sought-after elements. These elements are critical in ensuring that numerous daily needs of our modern technology-powered society are fulfilled (Balaram, 2023). REEs possess distinctive optical, electrical, magnetic, and luminescent properties, making them indispensable and critical elements globally (Balaram, 2019). REEs are behind the fourth Industrial Revolution (4IR)-driven digital technology. Their exploration of emerging technology such as electric vehicles, energy-efficient lighting, catalytic converters, flat-screen televisions, and disk drives is quite considerable.

Contrary to what their name suggests, rare earth elements are often spread across the crust due to their geological properties they are typically not found in concentrated clusters but rather are enriched to ore levels by conventional geological processes. REEs are categorised into two groups based on their atomic numbers, the lower atomic numbered are light rare earth elements (LREEs), while the higher atomic numbered REEs are categorised as heavy rare earth elements (HREEs) . The elements with the lowest atomic masses, lanthanum (La), cerium (Ce), praseodymium (Pr), neodymium (Nd), and samarium (Sm), are categorised as light rare LREEs and have atomic numbers 57-62. The HREEs which include europium (Eu), gadolinium (Gd), terbium (Tb), dysprosium (Dy), holmium (Ho), erbium (Er), ytterbium (Yb), Thulium (Tm) and lutetium (Lu), are the least common but most precious elements between atomic numbers 63 and 71.

Yttrium (Y) and Scandium (Sc) share similar physicochemical properties with the fifteen lanthanides, and they are defined as rare earth elements by the United States Geological Survey, USGS 2014 and the IUPAC. Promethium (Pm) is generally disregarded as an element due to its unstable nature while Ce has proven to be more prevalent and abundant than copper and gold in the earth's crust. Haque and co-workers (Haque et al., 2014; Zhang and Hu, 2019)also state that even those considered rare in the group of REEs are more abundant than gold.

The United States (US) government have declared the REEs as economically critical elements because (i) they possess unique properties, making them indispensable, (ii) are of geological scarcity, (iii) at risk of potential supply constraints, and (iv) are unreasonably high in price (Bobba et al., 2020). Rare earth elements can be categorised based on the demand, ranging from critical rare earth elements (Dy, Eu, Nd, Tb, and. Y), to excessive rare earth elements (Ce, Ho, Tm, Yb, and Lu) to uncritical rare earth elements like Pr, La, Gd, and Sm (Seredin and Dai, 2012).

Of the world's 120 million metric tons of REEs, China possesses 44 million metric tons, pushing for secure supply outside of China (Jowitt, 2022). Due to the environmental impacts and declining prices of the REEs in 2003, the Mountain Pass mine halted the mining operations. The change negatively impacted the rare earth life chain in the USA, leading to significant REE applications decline by 29% between 2004 and 2005 (Alam et al., 2012), the decline in USA rare earths supplies led to increased global demand. By the 2010s, nearly 85% of the worldwide supply including 95% of processed REEs was from China, countries became dependent on China's export (Walters, 2011). Because of its effective methods and technology for extracting and purifying REEs from minerals, China dominates the markets. China is the world's most populous country, meeting the international export demand and its own local supply placed China in a predicament. The

worldwide supply and demand of the technology materials was impacted compelling countries outside of China to search for other supplies. The implementation of the export restrictions of rare earths resulted in rapid escalation of the metals prices between 2010 and 2014 (Morrison and Tang, 2012).

Analysis according to USGS, 2022, around 44 metric tons of REEs are lying dormant in Chinese soil, with Vietnam as the second largest pile at 22 metric tons while more than 20 metric tons remain unexplored in Brazilian and Russian grounds. About 61% of all REEs mining production worldwide comes from China, thus most of these elements traded on global market (as shown in Figure 1.1), and the second largest producer has relatively small market share of about 15.5%. Currently REEs are not mined anywhere in Europe, with an estimation of 98% of REEs used in the EU imported from China (Armstrong, 2023).

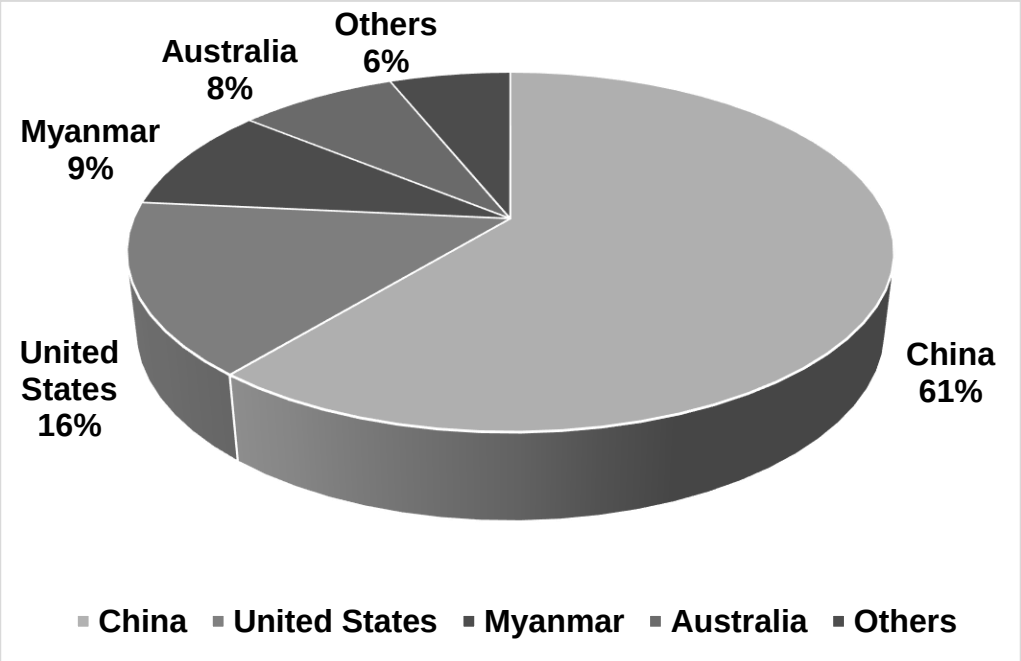

Figure 1.1 China dominates in the global production of REEs in 2021, adopted from www.statista.com accessed 29.07.2024

The Australian Mount Weld and Mountain Pass have increased REEs production, with countries like South Africa, India, Vietnams, and Kazakhstan planning to begin (Balaram, 2023). The challenge with REE supply scarcity is worsened by these elements not occurring in an equal or even distribution that is predictable (Moila, 2019). According to Oddo-Harkin's rule(Gupta and Krishnamurthy, 2005), the even numbered atomic REEs are substantially more prevalent than their neighbours in the periodic table within the earth's crust.

Rare earth elements' reactive nature prohibits them from existing individually like silver, copper, and gold that are native metals. Numerous minerals including oxides, silicates, phosphates, and carbonates host the metals as either major or minor constituents (Balaram, 2023). REEs are not conforming to the structure of most minerals and thus only present in a few geological environments. Only three of the 200 most well-known minerals containing rare earths, are mineable with significant economic value, the bastnaesite, monazite, and xenotime (Bezerra de Oliveira et al., 2019). Monazite is vital in petrogenic and geochronological studies, also used in the age dating of igneous, metamorphic, and diagenetic environments. The mineral is the primary source of light lanthanides, uranium (U) and thorium (Th) (Xaba et al., 2018).

Several beneficiation processes, including mining, milling, separation, purification and refining are involved in the production, sale and the use of REEs from the mineral sources. Hydrometallurgical procedures will be utilized to recover rare earth metals (REM) following the production of rare earth concentrates through flotation, beneficiation by gravity or magnetic methods, and ore mining. The highly effective separation technologies have been developed to produce high purity REEs from the mineral constituents. To separate U and Th, monazite is chemically treated with sodium hydroxide (NaOH) while sulfuric acid (H_2SO_4) cracking is necessary to recover rare earth elements as rare earths sulphates.

Rare earth elements are essential for sustainability and advancement of green energy solutions. Furthermore, South Africa possesses rich deposits of monazite mineral sources, and the scientific research is essential to address the inadequate analytical skills required for accurate analysis of elemental concentrations of REEs.

1.2 Problem statement

The growing global demand for rare earth elements (REEs) is being driven by the need for clean energy technologies (such as electric car batteries, wind turbines, and magnetic levitation trains) as well as advanced military hardware. These technologies are critical to the future geopolitical landscape, making REE extraction and analysis more crucial. The mineral monazite is one of the most important sources of REEs, but the challenges connected with its processing and analysis pose a crucial challenge. In addition, Monazite (a phosphate-rich) mineral found in beach sand placer deposits and igneous rocks, contains high levels of essential REEs but is difficult to process due to its complicated composition and the severe extraction conditions (Orris and Grauch, 2002). Monazite mineral is a typical beach sand placer mineral it is found in the vein deposits and acidic igneous rocks mainly comprising of 24% of phosphate (P_2O_5), 55-60% of metal rare metal oxides (TREO), 5-10% of thorium oxide (ThO_2), and less than 1% uranium (U_3O_8). The fundamental concern is the environmental and analytical challenges presented by current technologies for extracting and analysing REEs from monazite. The extraction method often uses corrosive acids and high-temperature flux fusion, which can cause substantial environmental damage, including the discharge of hazardous by-products like thorium and uranium. Furthermore, the complex chemical features of REEs, particularly the comparable behaviour of light LREEs and HREEs, make it difficult to separate and measure. This poses substantial difficulty in estimating the concentrations of these elements, particularly HREEs, using standard techniques such as ICP-OES (Scherrer et al., 2000). The high concentration of LREEs causes spectral interferences, making it difficult to reliably quantify HREEs at lower concentrations. The implications of such challenges are far-reaching. Mining businesses

involved in REE extraction are impacted by present technologies' inefficiency and environmental effect, resulting in increased operational costs and regulatory demands. The green energy and technology sectors are likewise limited in their availability of REEs, which could postpone widespread acceptance of clean energy solutions and impede the shift to sustainable energy. Furthermore, the defence and military industries rely on a consistent supply of vital REEs for advanced armament and defence systems, and any disruption in this supply could have major implications for national security(Balaram, 2023). Furthermore, the current techniques of extraction and processing pose a danger of pollution and long-term environmental damage to populations near mines. The efforts have been undertaken to solve these difficulties, such as researching more ecologically friendly extraction processes and developing new analytical procedures. For example, different solvents and chemical procedures are being investigated in order to lessen the environmental impact of REE extraction (Xaba et al., 2018). Furthermore, advances in analytical procedures such as spectroscopic techniques are being investigated in order to overcome the limitations of ICP-OES. However, these ideas have not yet been extensively implemented or shown to be economically viable on a big scale. Additionally, Preparation of monazite samples for the analysis using inductively coupled plasma techniques is extremely challenging as harsh conditions, including the use of corrosive mineral acids as well as high temperature flux fusion are required. The sulfuric acid fuming may not fully decompose the trace amounts of related minerals such as of related minerals, including zircon, ilmenite, rutile, garnet, and sillimanite that are frequently present in monazite samples (Padmasubashini, 2022). The heavy interferences in ICP-OES, and furthermore the ratio of LREEs to HREEs is extremely high in monazites hindering the accurate determination of very low concentration of HREEs (Eu-Lu)

due spectral interferences (Premadas.and Khorge, 2006). If these issues are not addressed, the consequences may be catastrophic. The environmental degradation will persist, posing long-term ecological and health dangers to the communities involved in REE extraction. The worldwide transition to clean energy may be delayed, impeding the advancement of green technology and affecting economies that rely on these breakthroughs. Geopolitical conflicts may also escalate as governments struggle for access to restricted REE resources; countries that fail to develop sustainable extraction methods will continue to rely on a few global actors for supplies. This might disrupt supply chains and cause global economic imbalances.

1.3 Motivation for research

Analytical chemistry is important and through the geological mapping, mining, exploration, ore processing and even metallurgical processes. Through all these stages, accurate and precise data for the mineralogical, isotopic, and elemental concentrations of REEs is required. The advancement in analytical techniques and performance has drastically improved in over a decade, however sample digestion methods are lagging and more often a bottleneck.

In most cases, the sample matrix's complexity will influence the choice of digestion method and analytical technique to match the requirements of the analytes. Complete sample dissolution is very critical for accuracy and precision of elemental and isotopic composition. Challenges associated with the REE bearing mineral monazite is its refractory nature, which requires the use of corrosive mineral acids or elevated temperature during the flux fusion for complete sample dissolution. Value addition of the study comes from selecting appropriate and effective reagents that ensure complete sample dissolution, with minimal contamination, reduced

consumption of reagents. The effective sample technique that can be rapid, easy to follow, and is practical for high sample throughput which is a basic requirement for geochemical laboratory and cost effective.

1.4 Aim and Objectives

The study aims to develop a method for quantitative determination of REEs in monazite samples using spectroscopic techniques.

- To develop a dissolution method that will ensure total sample dissolution for optimum REEs extraction:
- Optimise and evaluate analytical technique for measurement of rare earth elements.
- Compare the analytical results using the statistical evaluation.

1.5 Hypothesis

The use of the optimum and rapid sample digestion method will yield the high recoveries ~100% of REEs in monazite without the pre-concentration and selective precipitation steps. The optimized analytical technique, like ICP-MS or ICP-OES, can provide high precision and accuracy in measuring REEs, with recovery rates approaching 100%. This can be tested by comparing results with reference materials or validated techniques.Additionally, Statistical comparisons like ANOVA or regression analysis can verify the uniformity of REE concentrations and compare the precision of the optimized method to traditional techniques.

1.6 Research question

- Are the REEs in the monazite matrix accurately quantifiable without the preconcentration and REE selective separation/precipitation procedures?
- Which sample preparation method is efficient for the high recovery of the REEs (flux fusion or acid digestion method)?
- Which analytical technique is sufficiently sensitive to detect the REEs in the monazite matrix between ICP-OES and ICP-MS?
- What are the advantages and constraints of direct determination of REEs in a monazite matrix?
- Will the use of the developed method have any impact on the costs and time required for the REEs analysis in monazite?

1.7 Dissertation layout

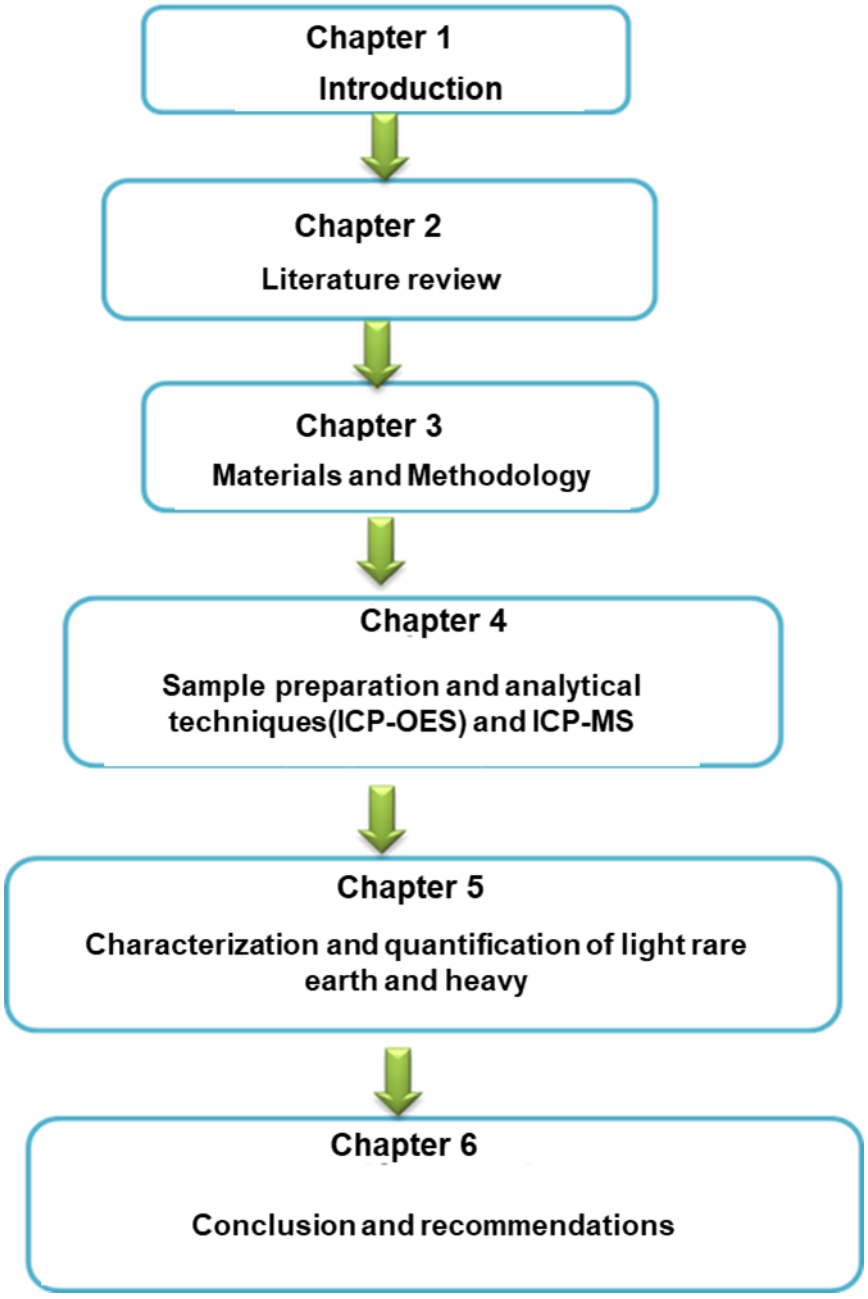

Figure 1.2 Dissertation layout showing the sequence of the chapters.

CHAPTER TWO: LITERATURE REVIEW

This chapter encompasses a thorough assessment of the literature that starts with the history of REEs, their significance worldwide and in modern-day technologies, their various deposit types, and their distribution around the world. An outline of the chemical and physical techniques employed for the extraction of REEs. The importance of the integrated mineral characterization methods as decision-making tool in the rare earth mineral exploration.

2.1 The Discovery of the rare earth elements

Though the rare earths have been in existence since the beginning of time, it was only until the late 18th century that their existence gained recognition when a Swedish mineralogist, Carl Alex Arrhenius discovered an unusual black mineral named ytterbite. The mineral sent to Johann Gadolin, who later renamed the sample gadolinite, and found numerous HREEs in the sample. Over time the exploration led to the discovery of yttrium, ytterbium, terbium, and erbium because of the academic exercises aimed at identifying new elements, when the REEs separation and isolation procedures began(Greinacher, 1981). In the early 18th century, cerium was independently discovered by European chemists Wilhelm Hisinger and Jöns Jacob Berzelius in Sweden and German-based Martin-Heinrich Klaproth from a reddish-brown mineral called cerite. In 1825 Mosander and Berzelius adopted a protocol from Ørsted where cerium chloride was reduced to form metallic cerium, leading to subsequent discoveries and naming of lanthanum, terbium, erbium from the cerite in 1839 by Mosander (Greinacher, 1981).

Around 1859, Robert Bunsen and Gustav Kirchhoff developed the spectroscope for elemental determination, which motivated the study of REEs. In the next fifty years, the number of REEs increased to fifteen creating a challenge for Mendeleev's periodic table as shown in Figure 2.1, requiring modifications simply to accommodate the rare earths, isolation of REEs remained the greatest challenge then and now (Greinacher, 1981).

In 1880s, Carl Auer Welsbach, a student at Heidelburg University under the supervision of Robert Bunsen discovered as well as isolating didymium as an alloy with neodymium and praseodymium, leading to the first commercial use of REEs. A gas mantle that produced light (as illustrated in Figure 2.2) was created after discovering the incandescent properties of REEs, producing five billion mantles. However, he was left with RE waste when

difficulty in lighting of the lamps arose, posing fire risks. Ferro-cerium was created by mixing the waste with iron, sparked by strikes and used in cigarette lighters and ignitions, with ore sourced mostly in countries like Brazil, North Carolina, and India creating the first recognised international REE trade (Greinacher, 1981).

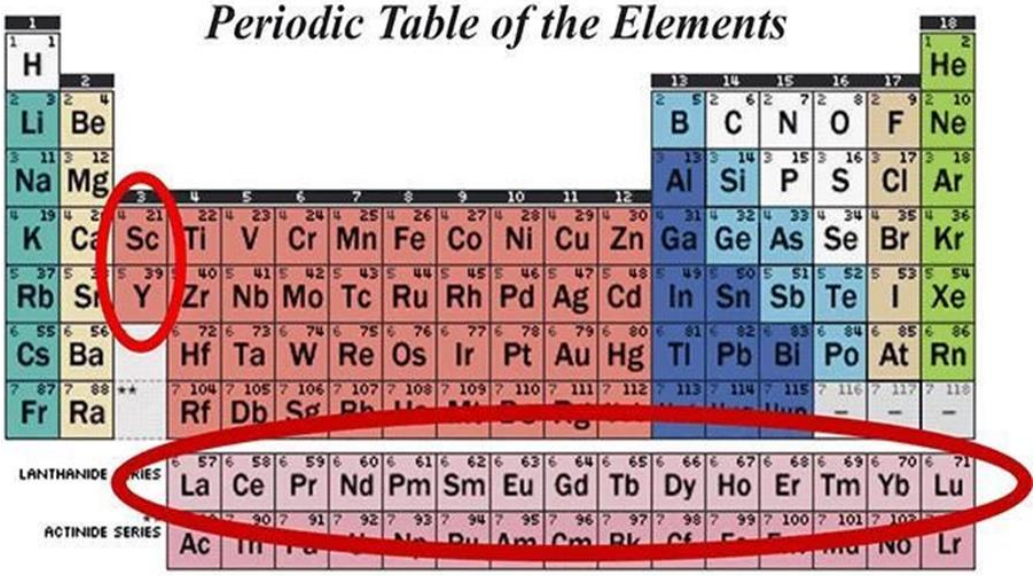

Figure 2.1 The periodic table by Mendeleev illustrating the lanthanides, Y and Sc circled in red. Adopted from www.efficientenergyllc.com accessed 29.10.2024

.

In 1907, Charles James, Carl Auer von Welsbach, and Georges Urbain separated Ytterbium into two fragments and named the lutetium (Lu) as the new element. Element 61 was discovered after the cation ion exchange, a new separation technique developed in the aftermath of the atomic bomb from the World War II (Greinacher, 1981). Promethium (Pm), named after the Titan who stole fire from the gods, the unstable element 61, it was in 1974 when the discovery of Pm was finally announced by Marinsky and Coryell.

Figure 2. 2 Example of the petroleum vapour lamp with an unburnt mantle. Source (Etan J. Tal)

2.2 Rare earth (REEs) bearing minerals and ores

Despite their relative plentifulness within the crust of the earth, the rare elements are not uncommon contrary to their name, they are rarely concentrated in deposits of economical viable ore. The light REEs or heavy REEs are typically found in minerals as the main lanthanides, which is due to the easy displacement/ exchange of elements that are similar in ionic

radii. The phenomena of ion displacement results in minerals enriched either in LREEs or HREEs (Xaba et al., 2018).

To date there are over 200 rare earth bearing-minerals from various types of deposits also found in all minerals (carbonates, silicates, oxides, hydroxides, fluorides, and phosphates (Balaram, 2019).The most economically viable minerals for the metal recovery and beneficiation include bastnaesite, xenotime, and monazite (Gupta and Krishnamurthy, 2005). Generally, LREEs are less expensive as they are more abundant that HREEs. Due to their greater abundance, LREEs are typically less expensive than HREEs. Even atomic number elements such as Ce, Nd, Sm, Gd, Dy, Er, and Yb are abundant than odd atomic number metals such as La, Pr, Eu. Tb, Ho, Tm, and Lu (Seredin and Dai, 2012).

The mineral deposits of REEs are classified as secondary or primary. The hydrothermal and igneous process are associated with the primary carbonatite, while the weathering and sedimentary processes are related to the primary carbonatite (Sappin and Beaudoin, 2015). The primary deposits comprise of the following (i) carbonatites and alkaline igneous rocks (ii) Skarn deposits (iii) Pegmatites (iv) Iron ore oxides, copper-gold deposits (iv) Vein deposits, and others (Gupta and Krishnamurthy, 2005). Currently, the main REE deposits are in India Brazil, Russia, Canada, Vietnam, South Africa, China, and Namibia. Recent years have seen the successful discovery of new REE deposits in few other nations such as Australia, Türkiye USA, and Sweden with China remaining the world’s largest producer at 97 % (Balaram, 2023). The major global REE deposit locations indicated in Figure 2.3 shows how the primary deposit, carbonatite dominates globally.

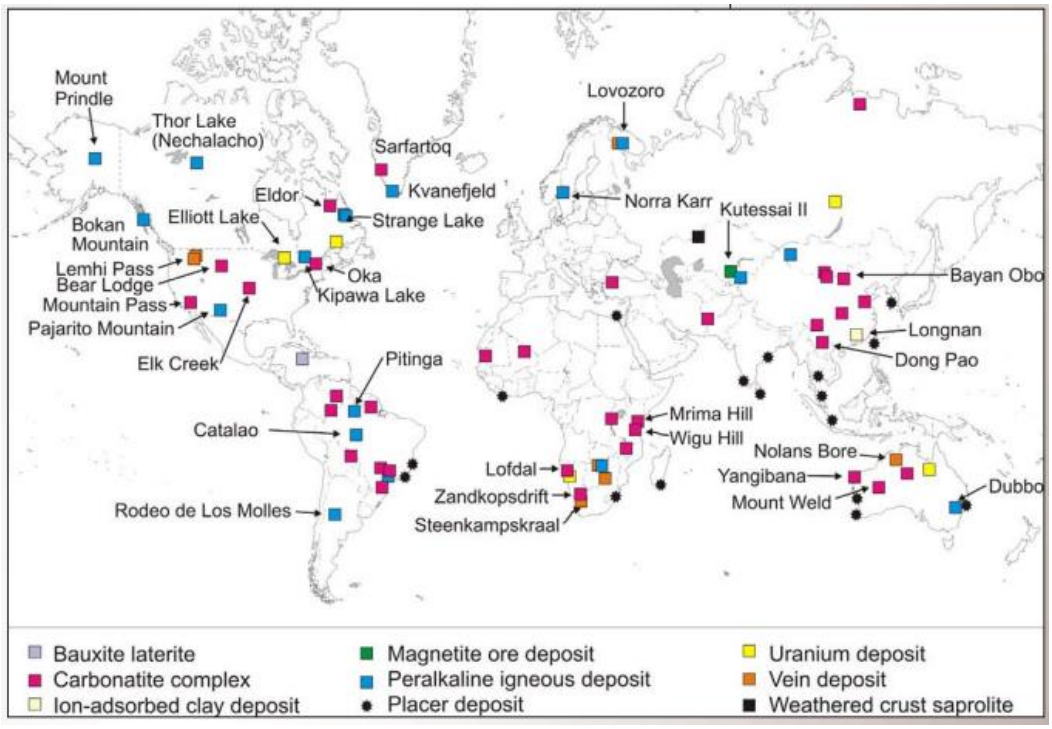

Figure 2.3 The major global REE deposit locations. Image adopted from Mariano and others, 2010)

2.3 The mining history of monazite mineral

After von Welsbach made the initial discovery of monazite sand in the 1880s while searching for thorium, the sand gained recognition and the REE trade was established. South Africa, Brazil, Australia, North Carolina, and India are the countries with the monazite deposits. Monazite was the most significant source of commercial REEs, however, because of the issues with the handling and disposal of radioactive material. thorium bastnaesite displaced monazite as the primary source of REEs. During the weathering of pegmatites, monazite minerals are more concentrated in alluvial sand due to their high density. Since the accumulation is the result of gravity separating from a particular source rock during the sedimentary process, the deposits are classified as placers (Sen Gupta & Bertrand, 1995). There are various kinds of placer deposits, such as beach placers, eluvium, alluvium, and paleo-placers replaced the mineral in the 1960s as the primary rare earths source because of its high Th content.

Beach placers are generally dominated by heavy minerals including rutile, zircon, ilmenite, and magnetite in varying proportions. Because the monazite contains variable structures, it is therefore classified as a collection of minerals with Ce monazite as the dominating group. Monazite is primarily reddish in colour, and typically occurs in tiny segregated crystals, on Mohs scale of mineral hardness, monazite measures 5.0 to 5.5 of hardness, and is dense at around 4.6 to 5.7 gram per centimetre g/cm^3 (Zaman, 2015). Monazite sand deposits are rich in common monazite (Ce) composition, typical composition of such lanthanide contains about 45-48% Ce, about 24% La, approximately 17% Nd, approximately 5% Pr, and minor quantities of Sm, Gd, and Y. Europium concentration tends to be below 0.05%. During the 1950s and 1960s, the South African monazite mined Steenkampskraal deposit was the biggest producer of REEs, with a full spectrum of lanthanides. Thorium content in monazite varies, it can be up to be 20-30%, however the Bolivian tin ore veins are supposedly Th free (Orris and Grauch, 2002).

Placer deposits comprise minerals with a specific gravity greater than 2.58 grams per cubic centimetre (g/cm3). The most prevalent non-economical minerals, such as quartz are washed away, leaving behind minerals like monazite. This property that sets the monazite apart, by virtue of their hardness, placer minerals can withstand abrasion during transportation and mechanical breakdown. For a mineral to withstand chemical breakdown of the mineral it must possess stability making the chemical breakdown of the mineral extremely difficult. Rivers or other coastal processes naturally transport and deposit heavy minerals beach sands alongside sands and gravel processes. Monazite is the most significant REEs containing mineral in this kind of deposit, although xenotime may sometimes occur in trace levels (Orris and Grauch, 2002).

Carbonatite contains a variety of minerals including monazite, synchysite, bastnaesite and allanite, which is the primary source of light REEs. Igneous

rocks that have a strong magmatic origin are associated with carbonatite, they have low levels of silica and elevated levels of carbon dioxide. Invading and solidifying within the crust of the earth (Sen Gupta and Bertrand, 1995). Over 500 carbonatite deposits have been documented worldwide including Prokusu (Namibia), Ambar Dongar (India), Barra do Itapirapua (Brazil), Bayan Obo (China), Mountain Pass (USA), Iron Hill (USA). Although hydrothermal deposit are not related to igneous rocks, they are a component of primary deposits and are rich in HREEs mineral like xenotime (Orris and Grauch, 2002).

Bastnaesite, laterite clays, monazite, and loparite, mostly mined as the sources of REEs, apart from the laterite clays which contain the HREEs and Y, approximately 95% of these elements are contained in these minerals as they are good sources of LREEs. Minerals such as apatite, euxenite, gadolinite, and xenotime, as well as allanite, fluorite, perovskite, sphene, and zircon are minerals that contain rare earth elements, from which REEs can be recovered from as by-products of mineral processing and deep-sea muds (Greinacher, 2024). The amount of REEs, Th, and U in monazite across the world differ from location to location depending on the monazite mineral type. Because of the refractory nature of monazite, leaching techniques involving corrosive chemicals are commonly employed in the extraction of REEs, however , the process’s effectiveness depends on the mineralogical and chemical characteristics of the particular monazite concentrate (Gupta et al., 2015). The mineral’s phosphorus content ranges from 24.5 to 30 % depending on the geological setting from which it formed, with the mineral as the primary source of light lanthanides. Monazite is typically extracted from other related heavy minerals in beach sand using gravity and electro-magnetic separation techniques (Gupta .et al., 2015).

2.4 Recovery and separation processes for rare earth elements (REEs)

Leaching, ion exchange, solvent extraction, and precipitation techniques have all been often employed to separate rare earth metals from monazite. Concentration, physical separation, and beneficiation are used interchangeably in extractive metallurgy to describe the ore treatment with the intention of increasing the fraction of the desired mineral concentration (Kumari et al., 2015). While the beneficiation (as shown in figure 2.4) is done by removing the undesirable ore constituents, also known as gangue, the concentration of REE mineral can be achieved in numerous ways based either on physical and/or chemical properties. The gangue and REEs containing minerals differ in terms of their electrical conductivity, floatability, magnetic susceptibility, specific gravity, and even how they react to physical and /or chemical processes (Kumari et al., 2015).

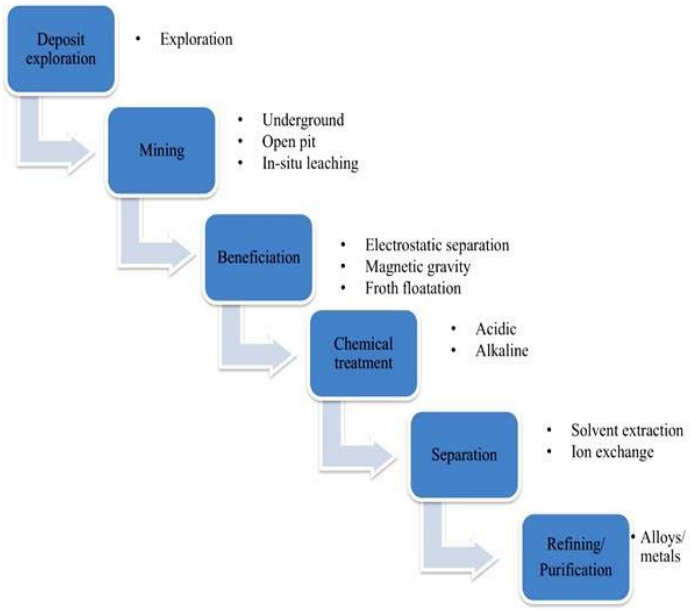

Figure 2.4 A typical flowsheet outlining steps until the final refined product for specified downstream applications

The magnetic separation method uses powerful magnets to either enrich or produce monazite or xenotime concentrate, rejecting non-magnetic gangue, and this stage is normally very efficient for monazite because of their paramagnetic properties (Gupta and Krishnamurthy, 2005). Monazite from placer deposits exhibits strong paramagnetic properties, react well to gravity and magnetic separation methods, while the heavy mineral waste containing rutile and zircon are rejected. Zhang and Edwards, (2012) used the magnetic separation for beneficiation of Chinese bastnaesite, rejecting the iron (Fe) bearing gangue mineral prior to REE isolation and purification., and floatation method was more suitable for fine grains size (100 μm) (Zhang et al., 2012).

The gravity separation method is best suited for concentration of ores with dense specific gravity from the lighter gangue by allowing the mass to flow with water. The beach placer rare earth bearing mineral possess dense specific gravities ranging between 4 and 7, making this separation method the best option, however the disadvantage arise when the specific gravity of both the undesired gangue and the desired minerals is equal. The separation method is beneficial for monazite recovery as it is less costly, and the beach sand have a wider range of specific gravity (Ferron et al., 1991).

Liberation of rare earth elements from their carrier minerals involves two processing routes: acidic and alkaline, where the already upgraded material undergoes either route based on mineralogy. In contrast with caustic soda cracking, the sulfuric acid leaching or acid baking is an-economical method for the extraction of REEs (Chin.and Wang, 1996). The method involves directly decomposing monazite using the sulfuric acid at temperatures between 200-400°C, for the ultimate conversion of REEs into rare earth sulphates REE (SO_4) with the SO_4^{2-} acting as a suitable ligand at elevated temperature. The leaching procedure has a significant drawback in causing the formation of double sulphates, which affects REEs purification, and the

phosphate binding of monazite does not immediately separate (Kumari et al., 2015).

Another technique for REEs extraction is the alkali fusion, the procedure involves employing sodium hydroxide to break down the monazite phosphate ion at elevated temperature and pressure combined. At the temperatures ranging from 140 to 170° C, the mixture of the ore with about 50 to 70 weight percentage of NaOH is decomposed to get water-soluble rare-earth hydroxide, REE-(OH) (Kumari et al., 2015). Hydrochloric acid is mostly preferred for decomposition of carbonate minerals at temperatures above 90 °C, including other minerals such as parasite, bastnaesite, synchysite, cerite, gadolinite, and allanite. In fluoride-containing ores like bastnaesite, insoluble REE-fluorides remain in solid as residue, requiring further decomposition with sodium hydroxide and soluble sodium fluoride. Excess HCl dissolves REE hydroxides while fluorides are washed away, but undesired carbonate phases dissolve, leaving bastnaesite intact and requiring larger reagent consumption (Kumari et al., 2015).

2.5 Future forecast of rare earth elements

The need for rare earth elements is estimated to rise significantly in the next decade due to technological advancements and green energy solutions, but there are concerns involving supply chain issues and the environmental impact (Filho et al., 2023). The International Energy Agency (IEA) predicts the demand for rare earth elements to triple by 2040 and meeting the 2016 Paris Agreement's emissions reduction requirements would require quadrupling global mineral supply, and the current supply is only doubling (Filho et al., 2023). Rare earth elements and other essential metals are essential for the switch from fossil fuels to renewable energy sources by 2050.

The primary and secondary resources are depleting, and future supply is uncertain. As such extensive exploration, mining and extraction operations are required for consumer electronics, the low carbon energy transition and national security (Balaram, 2023). These metals are crucial, and as such it is evident that sustainable management strategies need to be put in place urgently while exploring other sources of REEs exploration (Filho et al., 2023).

2.6 Lanthanide contraction and the resultant effects on rare earth elements

Lanthanide contraction (as shown in Figure 2.5) is referred to a progressive decrease in size as the atomic number with increasing atomic number. As the atomic number increases, its atomic size steadily decreases, the reason for this rise is the rise in nuclear charge and the electrons entering the inner orbital shell. While the number of electrons increase in an inner shell, additional shell is not created resulting in atomic radius not changing. The atoms in the third transition series are nearly identical to that of the second transition (Cotton, 2006).

As the atomic radium decreases and the number of protons rise, there is a rise in ionization energy. For example, the atomic radius of Nb is equal to the atomic radius of Ta, while that of Zr is equal to the atomic radius of Hf. Separation of lanthanides become a challenge due their chemical properties are similar. Since the ionic radii of lanthanides only differ slightly, making their separation quite challenging. Lanthanides size decrease from La to Lu. lanthanum hydroxide La $(OH)_3$ is more basic than lutetium hydroxide Lu $(OH)_3$ as the hydroxides covalent character increases their basic strength reduce (Cotton, 2006).

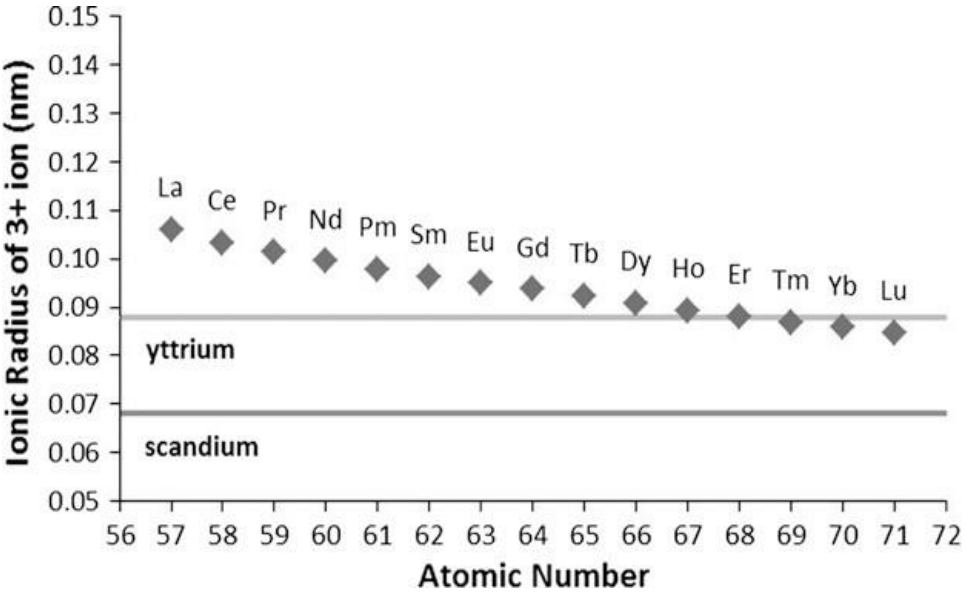

Figure 2.5 Lanthanide contraction, decrease ionic radii with increasing with increasing atomic. Adopted from literature by (Cotton, 2006)

2.7 Quantification aspects of the rare earth elements (REEs)

Analytical chemists face challenges in determining the REEs concentrations in monazite due to highly resistive nature and high thermal stability properties requiring aggressive chemical processes for the quantitative extraction of REEs, and most often these accessory minerals host heavier lanthanides such as Dy to Lu (Jarvis and Jarvis, 1992). Successful sample decomposition and appropriate analytical methods, equipment, and skills are crucial for accurate and reproducible quantification of REEs in minerals and ores. The first step in sample preparation involves sample decomposition with the aim to transform the elements of interest into a uniform soluble salt appropriate for chemical analysis using the specific analytical technique. Sample digestion is crucial for analysis and often it can limit sample throughput especially with modern advanced rapid multi-element determination techniques (Chao and Sanzolone, 1992).

While there isn't a single method that can dissolve every element in every type of geochemical samples, there are efficient techniques that can be developed for specific samples matrices and for selected group of elements. Most often, the complexity of sample matrix dictates the selection of a suitable sample digestion and the analysis methods, also there are factors to consider which include sample properties, elements of interest, sample size, residue matrix suitability, sample throughput, precision, available laboratory facilities, reagents costs, and operational skills. There are various sample digestion/dissolution methods available for the geological and environmental samples (Chao.and Sanzolone, 1992). Monazite is chemically stable to withstand the weathering (Hu and Qi, 2014), to successfully destruct this mineral for liberation of the REEs, high temperatures flux fusions and corrosive minerals acids are employed most often for total sample dissolution during REEs determination by ICP-OES and ICP-MS (Murty et al., 1990). Minor quantities of associated minerals like zircon and others, which may contain HREEs might be partially decomposed during the sulphuric acid fuming technique at 250-300 °C for 2-3 hours resulting in inaccurate REE recoveries (Radhamani et al., 2007) requiring subsequent sample fusion using either phosphate and/or fluoride salts (Xaba et al., 2018).

Strong mineral acids hydrofluoric (HF), perchloric ($HClO_4$), sulphuric (H_2SO_4), nitric (HNO_3), phosphoric (H_3PO_4) and hydrochloric (HCl) acids are typically used to dissolve different types of samples including rocks and minerals which have been effectively decomposed using the appropriate acid combinations (Jarvis and Jarvis, 1992). Given that all the above-mentioned acids are naturally destructive particularly when hot and undiluted, extreme caution is required to prevent injuries (Hu and Qi, 2013) The properties of the routinely used mineral acids are enlisted in the Table 2.1.

Table 2.1 Common mineral acids and their physical characteristics for sample preparation of REEs (Hu and Qi, 2013)

Mineral acid	Formula	Molarity (M)	Concentration	Density	Boiling point (°C)
Hydrochloric acid	HCl	12	37	1.19	110
Hydrofluoric acid	HF	29	48	1.16	112
Nitric acid	HNO_3	16	68	1.42	122
Perchloric acid	$HClO_4$	12	70	1.67	203

The mineral acids (HF) can effectively transform silicates by dissociating the strong Si-O bonds into volatile silica tetrafluoride SiF_4, which evaporates during the open vessel acid digestion process (Hu and Qi, 2014). Almost always, in combination of HF and other acids including $HClO_4$ and/or HNO_3 to provide complete sample dissolution by obtaining the homogenous high oxidation state solutions, since the acid etches glass even diluted, the use of Teflon or polytetrafluoroethylene (PTFE) is a required (Hu and Qi, 2013). Since it is a weak reducing agent, hydrochloric (HCl) is not preferred for the digestion of organic materials but utilised frequently for geological samples dissolution. The chloride ion (Cl^-) have complexing abilities and reducing properties, making the acid an excellent choice for the dissolution of phosphates and carbonates. Due to chloride induced poly-atomic ions causing significant interferences, HCl is not recommended as the final sample solution in ICP-MS analysis since it results in major interferences such as hypochlorite (ClO), hypochlorous (ClOH), argon chloride (ArCl) (Jarvis and Jarvis, 1992). One of the strongest acids, $HClO_4$ has strong dehydrating and oxidizing properties making it one of the strongest acids especially when hot and undiluted, and highly explosive when reacting with organic compounds. The perchlorate salts are extremely stable and soluble in water. Spontaneously flammable perchlorate salts require the utilization

of a fume-hood with wash-down mechanism (Chao and Sanzolone, 1992; Jarvis and Jarvis, 1992).

Nitric acid (HNO_3) is a strong oxidising agent that is capable of liberating trace elements from a rock mineral during sample preparation especially when hot and concentration. It is used to decompose the carbonates and sulphide minerals, and the nitric acid matrix is best suited for ICP-MS analysis since it comprises of the nitrogen (N_2), hydrogen (H_2), and oxygen (O_2) already present in the plasma entrained air. The addition of the acid during digestion does not increase polyatomic ions, as such does not interfere with most determinations (Hu and Qi, 2013). The products of monazite concentrate treated with sulphuric acid are not very pure as the acid does react with many impurities which recently resulted in the process commercially replaced by the NaOH method, also the H_2SO_4 roasting is less environmentally friendly owing to the radioactive uranium (U) and thorium (Th) present in the leach residue (Helmeczi et al., 2016).

2.8 Classification of flux fusion methods used for geological samples dissolution

As stated by Yu et al. (2000). that flux fusion techniques are an alternative to acid digestion by providing quick and thorough decomposition of all minerals that comprise rocks and including the extremely resistant ones. The fusion technique combined with ICP-MS analysis have not been used much until recently due to large amounts of TDS and relatively high blank level. Relatively elevated temperatures are required to dissolve the flux salt into ionic liquid. (Bokhari and Meisel, 2017).

Additionally, fluxes such as the borates like lithium metaborate ($LiBO_2$), potassium tetraborate ($K_2B_4O_7$), lithium tetraborate ($Li_2B_4O_7$), carbonates such potassium carbonate (K_2CO_3), sodium carbonate (Na_2CO_3), hydroxides such as sodium peroxide (Na_2O_2), sodium hydroxide (NaOH),

potassium hydroxide (KOH), or fluorides including potassium bifluoride (KHF_2), sodium fluoride (NaF), ammonium bifluoride (NH_4HF_2) are used. Hydroxides flux such as NaOH, Na_2O_2, and KOH are recognised for the decomposition efficiency of silicates, requiring less time between (10-30 minutes) and relatively low temperature between (500-700 °C) than fusion with $LiBO_2$ and Na_2CO_3 (Seelye and Rafter, 1950).

2.8.1. Sodium peroxide sintering or fusion for geological samples decomposition

Sodium peroxide is a strong alkali flux oxidizer, which provide rapid decomposition of the silicates, zircon, tourmaline, monazites, cassiterites, and chromite's. Fusion or sintering with sodium peroxide, generally is applied with the sample to flux ration of 1:4 at the temperature of 480 °C ± 20 °C for 30 minutes in a muffle furnace (Seelye and Rafter, 1950). The fine powdered sample will be thoroughly mixed with Na_2O_2 before heating using either open flame or high temperature muffle oven. The major role of sodium peroxide sintering or fusion is to destruct sample into a solution with minimum salt content (Chao and Sanzolone, 1992; Hu. and Qi, 2014) and literature exists on studies suggesting different amount of sodium peroxide to recover the elements of interest. Nickel, iron, gold, platinum, and zirconium crucibles are used for dissolution experiments using Na_2O_2. Zirconium crucibles are not easily corroded/ attacked by the molten Na_2O_2 flux, and they can withstand temperature up to 700 °C during the fusion process. Following cooling, normally the resultant fusion melt is dissolved in either HCl or HNO_3 after addition of water to the crucible to dissolve the contents. The silicate rocks are efficiently dissolved using NaOH/Na_2O_2 mixture at lower temperature as opposed to carbonate fluxes (Hu. and Qi, 2014).

The report by Bokhari and Meisel, (2017) states that applying the 1:6 sample to flux ratio of finely ground 100 mg of sample and 600 mg of sodium

peroxide, sintered at the temperature of 480 °C in a muffle furnace for thirty minutes in glazed carbon crucibles. The resultant melt dissolved in cold water, followed by centrifugation of the solution to separate the REE hydroxide precipitate from the whole rock matrix. The REE hydroxide precipitate was dissolved in 3 mol/L^{-1} of HCl to also dissolve problematic magnetite while the supernatant was acidified and transferred into 100 mL flask. The technique was found to be easy to learn even by inexperienced analysts, and that separation of REE hydroxide from the whole rock matrix eliminated the higher total dissolved solid.

The sintering procedure employed by Cotta and Enzweiler (2012) involved the mixture of 500 mg of finely ground Na_2O_2 and 100 mg of sample in a glazed carbon crucible at 480 °C for 10 minutes. As stated by Yu and co-workers (2000), that an alternative to acid digestion is flux fusion, which offers prompt and complete destruction digestion of ores and rocks including the refractory ones. A careful transfer of the solution containing the (Fe, Ti)-hydroxide precipitate to a centrifuge vial was made to remove the silica and sodium matrix. (Longerich et al., 1990) attested that the procedure provides rapid determination of REEs, Sc, and Y but (Yu et al., 2000) cited the short comings of the procedure regarding the high field strength elements (HFSE) which do not completely decompose.

The recommendation of Taicheng and co-workers (2002) is the addition small amounts of iron (Fe) and titanium (Ti) to the samples before using the sodium hydroxide and sodium peroxide for fusion. When the melt cools, it was dissolved in water and brought to boil to remove the H_2O_2 (Taicheng et al., 2002). The heating step was found to improve the co-precipitation of the HFSE while entirely precipitating $Ti(OH)_4$ and $Fe(OH)_3$. (Meisel et al., 2002) reported the low recovery of niobium (Nb) and tantalum (Ta) using the aforementioned procedure. REEs other elements and the HFSE were able to be measured after mixing the supernatant and the dissolved hydroxides. The high melt viscosities hinder siliceous samples from rapidly

homogenizing during melting on the strip which pose problems during fusion (Nehring et al., 2007). REEs can be precipitated with fifty percent NaOH after fusing and dissolution with HNO_3 transforming the solution into a strong alkaline solution (Helmeczi et al., 2016).

2.8.2. Lithium metaborate $LiBO_2$ flux fusion for geological sample decomposition

The lithium metaborate ($LiBO_2$) is a non-oxidative compound readily accessible as a very pure reagent, capable of decomposing most accessory forming minerals in rocks. The $LiBO_2$ fusion is possible in platinum (Pt) crucibles for approximately 15 minutes at temperatures ranging between 950-1050 °C. The resulting melt is digestible in either nitric or hydrochloric acid medium but for the removal of silica (Si) and boron (B) from flux as volatiles fluorides, the melt was digested using a mixture of HF and HNO_3 to minimise total dissolved solids (TDS) in solution (Panteeva et al., 2003). The major drawback of the technique lies with difficulty in leaching off the alkali cake for dissolution, and the prolonged sample fusion process, and the use of ultrasonication method facilitate the alkali cake dissolution.

The study by Makombe and co-workers (2017), employed both the lithium meta-borate fusion and wet acid digestion procedures for the digestion of sediments samples for quantification of REEs using the ICP-OES with the aim to obtain the optimum parameters (Makombe et al., 2017). The more successful of the two digestion methods tried was flux fusion due to the capability of total sample dissolution as well as the easy-to-use automated fluxer fusion machine. It was established from the study that sample to flux ratio of 1:8 was enough to fully dissolve the samples and not deposit on the ICP torch. The optimal parameter for the signal intensities was keeping the nebulizer gas flow at 0.80 L/min and the speed pump at 35 rotations per minute (rpm) Method performance characteristics such as linearity, accuracy, LOD and LOQ detection and quantification limits and accuracy in

the absence or presence of the internal standard were established for the La, Eu, Gd, and Yb in the sediment samples (Makombe et al., 2017).

An improved lithium metaborate fusion was used by Panteeva and co-workers to dissolve felsic rock samples and analysed using ICP-MS. Method validation involved the use of Geological reference materials such as AGV-1, GSP-1, STM-1, G-2, and BCR-1. After the resulting alkaline cake was dissolved with HF, it was treated with HNO_3. The obtained experimental results from the developed method agreed with the published values. The precision of the method ranged between 0.44 to 2.07 micro gram per gram µg/g for middle rare earths (MREEs) and HREEs, Pr, Ta, and U, the detection limits were found to be between 0.021 to 0.24 µg/g and for LREEs, Rb, Sr, Zr, Nb, Ba, Hf and Th they were. Granites and felsic volcanic rock from Southern Siberia were determined using the suggested dissolution method. The drawback associated with the dissolution method are prone to contamination induces by possible impurities in the flux, the loss of elements as volatiles, and the high salt concentration in the final sample solution (Panteeva et al., 2003).

With the above been said, lithium metaborate fusion has been successfully used to digest diverse kinds of geological samples for the REEs measurement, and the method has been found to be rapid, easy, and provide complete sample dissolution and blanks can be reduced by further digesting the alkaline in hydrofluoric acid.

2.8.3. Hotplate assisted open vessel multi-acids digestion method for sample dissolution

Sample preparation by acid digestion method involves the complete destruction of the samples with the aid of mineral acids, with the source of heat as either microwave, heating block digester or hot plate and subsequent use of ICP techniques for the REEs measurement (Zuma.et al.,

2022). Open vessel is a low-pressure acid attack procedure, usually carried out in screw top vials or containers on a hotplate. In addition to evaporation with hydrofluoric acid, other mineral acids are also employed to convert fluoride ions to soluble salts.

Yokoyama and co-workers (1999) reported that the removal of fluorides is possible with the evaporation of samples solution repeatedly using $HClO_4$, as the yield of 100% recovery for REEs and other elements were obtained using this procedure, however (Yokoyama and Makishima, 1999) indicated that the removal of fluoride is often difficult. (Potts, 2003) reported that silica (Si) and fluoride (F) are typically volatilized to silica tetrafluoride (SiF_4) by heating the geological samples with HF either by itself or in conjunction with other acids above room temperature in an open vessel. The boiling temperature of perchloric acid, which is 203 °C, makes it easier to attack refractory minerals and remove fluorides, producing highly soluble perchlorates. This is contrast to HF, which has a boiling point of 112 °C (Yokoyama.and Makishima, 1999). REEs and Th might be entrapped in the stable and insoluble Ca-Al-Mg crystal lattice during precipitation leading to inaccurate recoveries (Boer et al., 1993). To mitigate the issues of these refractory phases, a smaller sample weight not exceeding 100 mg is recommended as well as avoiding total sample dryness during sample digestion process.

The removal of hexafluoro silicic acid (H_2SiF_6) can be achieved with heating of the solution in acidic media using excess HF. The resultant solution sample becomes more stable as Si tends to hydrolyse in solution and precipitate upon standing, the Si and F induced interferences in some photometric determinations are eliminated, the destructive activity of HF is neutralised, resulting in decreased salt content. Total removal of fluorides from the solution is often complex, which may often form insoluble fluorides leading to inaccurate recoveries, some authors have used boric acid

(H_3BO_3) to break down the insoluble fluorides by acting as a complexing agent (Potts, 2003; Zhang et al., 2012; Hu. and Qi, 2014).

The accuracy in direct ICP-AES determination of trace levels HREES in monazite mineral is a challenge because of spectral interferences as well as the shift in plasma excitation conditions when high levels of LREE and thorium are introduced. Although ICP-AES provides rapid as well as multi-elemental analyses of REEs with sufficient sensitivity, most often the effective performance is affected by complex spectral emissions as well as the severe interferences from the matrix elements. Hence the cation-ion exchange must be employed to separate the REEs from the sample matrix, as well as a careful wavelength selection (Ardini et al., 2010).

2.9 The principles of the ICP-OES

Through the nebulizer, the peristaltic pump delivers the solution sample to the spray chamber. The aerosol that is produced is guided into the argon plasma. After solids, liquids, and gases plasma is the fourth state of matter. High frequency alternating current is carried by a cooled induction at the end of a quartz in the ICP-OES producing plasma. Consequently, a new magnetic field is created, which causes the electrons to accelerate in a circular fashion. Ionization results from the collision of the argon atoms and electrons, creating a stable plasma.

At the temperatures of 6000-7000 kelvin (K), the plasma is incredibly hot, and in the induction zone, it can reach 10000 K. The sample gets dissolved, atomised, and ionised in the torch. Thermic energy that the electrons absorb causes the electrons to rise to higher excited state. As the electrons return to their ground state, energy is released to higher excited state. As the electrons return to their ground state energy is released as photon or light. The spectrometer measures the unique emission spectrum of each element. The concentration calculated by measuring the wavelength

intensity with calibration. Figure 2.6 illustrates a typical ICP-OES, which normally measures the light emitted by elements using optical spectrometer to produce different wavelengths.

.

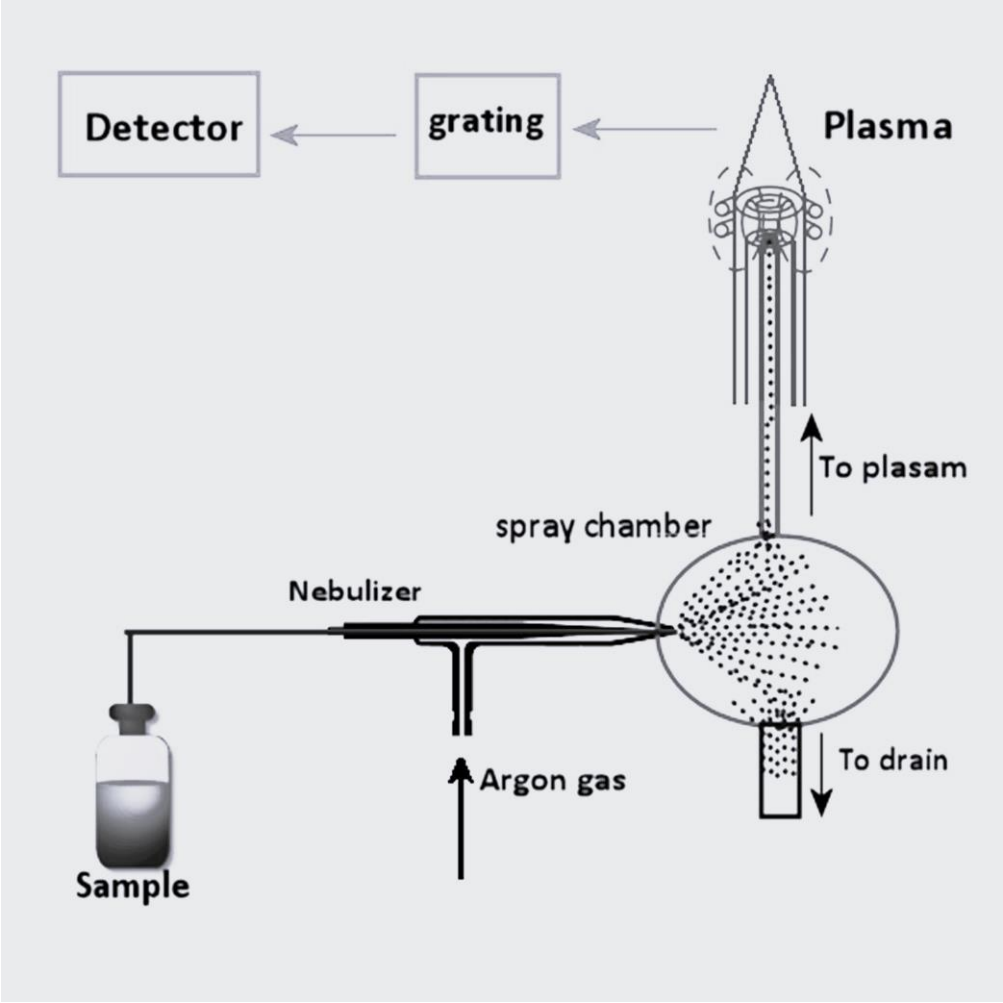

Figure 2.6 A typical illustration of the inductively coupled plasma optical emission spectroscopy. Adopted from literature by (Gouden et al.,2017)

Quality assurance is crucial in analytical chemistry as it plays an important role at ensuring correct analytical results are obtained. Accuracy and precision are sample digestion's two most crucial quality control metrics, as history has shown that most often it is the origin of errors (Hoenig, 2001). Precision and accuracy are the two most crucial control quality metrics for sample digestion. Precision is usually determined by calculating the relative standard deviation of duplicated analyses of the same sample, while accuracy measures the degree of to which the analytical data agrees with the true or assigned value of the sample. This assist in evaluating the

reproducibility of the same sample digestion. It is recommended to use appropriate reference materials for method development and quality assurance in sample preparation procedures, with certified values and traceable certificates from a valid certifying body. Certified reference materials (CRMs) are crucial in drift correction, secondary calibration verification, evaluating uncertainty and method bias measurements, instrument conditioning, control sample control charts, and assessing lab and analyst proficiency (Hu and Qi, 2014). Concentration range and matrix matching the samples are the two most crucial elements when selecting the CRMs to establish similar possible interferences (Meisel et al., 2002).

Selecting the appropriate internal standard in chemical analysis is crucial to manage random and systematic sources of uncertainties that may arise during sample preparation or instrument fluctuations and has been widely used. The internal standard also compensates for shifts in instrument sensitivity resulting from nebulizer, electronic drift, aerosol transport efficient, TDS content, including various other matrix effects. .Spiking of samples, calibration standards with a constant concentration of the internal standard been extensively applied in ICP-AES and ICP-MS (Jarvis and Jarvis, 1992).

For ensuring the suitability of internal standard element, there is a criterion used for selection such (i) the internal standard element is not an analyte (ii) the internal standard element possess similar properties as the analyte in terms of ionization energies and similar mass numbers (iii) the element not affected by matrix or spectral interferences (iv) and can be accurately measurable without affecting the instrument sensitivity, (v) does not contaminate the analyte. High purity standard solution such as indium (In), bismuth (Be), beryllium (Be), cobalt (Co), rhodium (Rh), gallium (Ga), tellurium (Te), and titanium (Ti) are often used once they are confirmed to meet the criteria (Jarvis and Jarvis, 1992). In this study rhenium (Re) and indium (In) were found to be suitable elements used for the internal standard

purposes. Lastly, selecting the proper sample portion before sample digestion play an important role in quality assurance. For the naturally occurring mineral, prior to chemical analysis sample preparation involving milling and pulverization to conveniently reduce the particle size is needed.

The grinding procedure enhances the effectiveness of the chemical analysis by aiding to increase the surface area and sample homogenization to ensure the aliquot taken will be a proper representation of the whole rock. SARM 148 was pulverised using a ball mill and reduced to particle size of 95% of the sample passing 75 microns screening sieve. The same procedure was then applied to the sample ZKD to ensure sample conditions are as similar as possible. For a particle size of level 74 milli-meter (mm) or 200 mesh it has always been recommended since the 1980s to use a minimum 100 mg test portion size to ensure proper sample representativeness of subsampling which is usually a compromise between the detection limits and sample size. The certified reference materials SARM 148 and IGS-36, were used in this study for method development, monitoring the sample preparation digestion as well as instrument performance. REE bearing monazite CRMs (SARM 148) were used to matrix match the monazite samples during optimization of the parameters. To trace the source of error, the procedural blanks comprising of the reagents used for sample digestion were prepared with each batch.

The certified reference materials SARM 148 and IGS-36, were used in this study for method development, monitoring the sample preparation digestion as well as instrument performance. REE bearing monazite CRMs (SARM 148) were used to matrix match the monazite samples during optimization of the parameters. To trace the source of error, the procedural blanks comprising of the reagents used for sample digestion were prepared with each batch. The appropriate sample analysis that ICP-MS and ICP-OES provide for a variety of elements with concentrations ranging from ppm to percentage levels makes them useful instruments in geological analysis.

However, it is challenging to measure higher concentrations due to the extreme sensitivity of ICP-MS, and to measure lower concentrations due to weak sensitivity of ICP-OES. Time and expense are critical in geochemical exploration since both methods necessitate sample preparation because they are solution based analytical tools. Both methods have benefits for geological research.

2.10 Overview of analytical characterization of REEs

The next step following the sample decomposition in analytical procedure is the quantification of the elements of interest using the preferred analytical technique. Spectrometric methods are widely used for quantifying elements of interest due to low running costs, low detection limits, easy qualitative analysis, simultaneous multi-elements analysis, and minimal chemical interferences (Jarvis and Jarvis, 1992). For precise elemental data, economical and quick analytical methods are needed for mining, exploration, geochemical mapping, ore processing, and metallurgical activities. Traditional techniques including spectrophotometric, gravimetric, and titrimetric methods are typically very difficult to employ to quantify REEs. Mainly because of their chemical and physical similarities, particularly in the matrix which can result in spectral and non-spectral interferences (Balaram, 2019). Isotopic mass spectrometry (IDMS) and neutron activation energy (NAA) have been the most favoured techniques for REEs determination in geological samples particularly due to their enhanced sensitivity. But they have drawbacks like time-consuming as well as prolonged and complex experimental procedures. Although the IDMS usually provides precise results, the major drawback is that it is impossible to quantify the mono-isotopic elements such Pr, Tb, Ho and Tm (Eggins et al., 1997).

Atomic absorption spectrometry (AAS) was utilized to quantify all the REEs, however the sensitivities are poor. ICP-AES or inductively coupled plasma atomic emission spectrometry has been employed to analyse REEs in ores

and geological materials rare earth concentrates (Parthasarathy.et al., 1986) and various geochemical material (Lichte et al., 1987).The first-time application of radio-chemical neutron activation (RNAA) was for analysis of all REEs with exception of Tm in Indian monazite.

As these more sensitive, accurate, and precise techniques developed, researchers began using multi-element techniques such as neutron activation analysis (NAA), x-ray fluorescence (XRF), ICP-MS, and ICP-OES, instead of flame absorption atomic spectroscopy (FAAS) and graphite flame atomic absorption spectrometry (GFAAS). These developed techniques were commonly used due to their higher sensitivity, low detection limits, wider linear dynamic range. The techniques also provide the accurate multi-element determinations and are less prone to both spectral and non-spectral interferences (Xaba, 2015) These techniques are currently extensively used for accurate quantification of REE contents in various samples contained in trace level concentrations range. It can be difficult to determine REEs in complex materials like minerals from both an instrumental and separation and/ or pre -concentration perspective, particularly when REEs are present at ultra-trace levels (Zawisza, et al*.,* 2011).

Rare earth elements are a coherent group, they share similar chemical and physical properties and often making their separation from each other or from their host minerals difficult, some authors have employed co-precipitation, solvent extraction precipitation, and chromatography are examples of separation and pre-concentration techniques that have been effectively used to enhance their accurate determination using various analytical techniques (Sen Gupta and Bertrand, 1995). The heavy thorium in complex monazite matrix causes physical and spectral interferences in ICP-OES, and furthermore the ratio of LREEs to HREEs is extremely high in monazites hindering the accurate determination of very low concentration of HREEs especially from Eu to Lu (Premadas and Khorge, 2006). Because

ICP-MS and ICP-OES are solution-based procedures, sample dissolution by wet chemical methods is both required and unavoidable.

2. 11 Studies on the chemical analyses on monazite ore

Study by Borai et al., (2016) which involved the use of complexing agents like oxalic and α hydroxyl isobutyric acids for the respective separation of LREEs, MREEs, and HREEs at ranging pHs and concentrations of eluent from sample matrix prior to quantitative determination of REEs in Egyptian monazite and xenotime, IGS-36 included using Ion Chromatography (IC) and ICP-AES. The monazite sample was digested using conventional sulphuric acid fuming procedure on the hotplate for 2-3 hours, the outcomes obtained by both ICP-AES and IC were in agreement with one another, with good accuracy (Borai et al.,.2016).

Click or tap here to enter text.The study by Padmasubashini and Satyanarayana (2013) involved two different samples decomposition methods for dissolution of Indian monazite and subsequent direct analysis using ICP-MS for REEs quantifications. A combination of sodium fluoride (Na_2F) and potassium bifluoride (KHF_2) was used for the flux fusion procedure, while acid digestion involved repeated steps of digesting the monazite with H_2SO_4. The results for IGS-36 results obtained by both sample dissolution methods for REEs, Y, U and Th compared well with each other and with the published values, except for the zirconium (Zr) value where higher recoveries were observed from the fluoride fusion digestion. The spectral interference of the LREEs on HREEs was corrected mathematically using using oxide yield and abundance data (Padmasubashini and Satyanarayana, 2013).

Another study by Padmasubashini (2020) involves the coupling of the conventional sulphuric acid fuming procedure with fusion of the residue using a mixture of fluoride flux for the simultaneous determinations of REEs,

Th, and P in Indian monazite using ICP-OES. Spectral interferences of LREEs and HREEs were resolved using correction factors as well as selection of suitable wavelengths without interferences. The relative standard deviation (RSD) for repeatability studies ranged between 2.6 to 10.2% while the RSD values for the intra-lab reproducibility studies ranged from 1.7 to 11.1% (Padmasubashini.et al., 2020).

Another study by Premadas and co-workers (2006) involved the solvent extraction procedure using bis-(2-ethyl hexyl) hydrogen phosphate (HDEHP) for separation of HREEs (Tb, Dy, Ho, Er, Tm, Yb and Lu) from Indian monazite matrix and direct determination of ICP-AES. Syenite rock (SY-3) and IGS-36 were used to check the recovery of HREEs, the RSD obtained for separation of HREEs, as well as the direct determination of Y, LREEs ranged from 1 to 7% (n=4) (Premadas and Khorge, 2006).

A novel method for the simultaneous determination of MREEs (Sm, Eu, Gd, Tb, and Dy) in the Indonesian monazite by combining ultraviolet-visible (UV-Vis) spectroscopy coupled with multivariate analysis was developed by Saputra and co-workers. The sample digestion method involved sample fusion in the flux mixture of sodium dibasic phosphate (Na_2HPO_4/ NaH_2PO4. H_2O.) sodium dihydrogen phosphate monohydrates. The chelating agents, biphenyl dicarboxylic acid and acetyl acetone were used for selective precipitation of REEs with lower detection limits of 1.375 (±0.012), 0.332 (±0.004), 42.117 (±0.200), 1.767 (±0.011), and 0.576(±0.002) ppm for Sm, Eu, Gd, Tb, and Dy, respectively. (Saputra et al., 2021).

The study by Xaba and co-workers includes the determination U, Th, LREEs (La, Ce, Nd, Pr, Sm) and Y from monazite after selective precipitation of REEs using the chelating agents such as biphenyl dicarboxylic acid and acetyl acetone before analysis using ICP-OES. The flux fusion digestion with a mixture of $Na_2HPO_4/NaH_2PO_4 \cdot H_2O$ rendered complete dissolution of the monazite sample. The REEs recoveries ranged between 90.2-101.68%

with RSD of 1-3% (Xaba et al., 2018). According to the literature, the flux fusion of monazite using fluorides and phosphates flux are most preferred for the total dissolution of the monazite samples. Furthermore, the separation of REEs from the sample matrix, or separation of HREEs, LREEs, or MREEs respectively from each other or from sample matrix at varying pH and concentrations of the eluents during chromatographic separation removes spectral interference and enhance the accurate detection of REEs during instrumental analysis. Near overlaps and spectral overlaps especially in matrices such as monazite have shown to complicate the trace level REEs analysis.

It is evident that interference removal techniques such as solvent extraction, ion exchange, selective precipitation are required, and finally the selection of alternative wavelengths with minimal interference are a resolution for accurate and precise determination of REEs by various spectroscopic techniques. ICP-OES is reported to be less sensitive especially towards trace level concentrations of REEs, as such it will be unfair to expect accurate results without matrix separation.

2.12 Emerging technologies and the use of rare earth elements (REEs)

The shift towards renewable energy and technological advancement are the key drivers increasing demand for the REEs. The demand is much more visible in various sectors such as electronics, auto-motives, and energy generation. The use of REEs in computers has increased at a rate that is comparable to that of cell phones, The demand for portable devices such as cell phones, portable computers, monitors, and cameras is driving the demand for rechargeable batteries, many of which are composed of RE components.

The distinctive characteristics of REEs allow them to enhance the performance of other metals in most cases resulting in reduction of the

amount of metal necessary for application. Smartphone uses about seven rare earth elements for everything from its coloured screen to the speakers, as well as the miniaturization of the phone's circuitry (Balaram, 2023). The Neo or neodymium iron boron (NdFeB) permanent magnets are made from Nd alloy, B and Fe. The naming only considered the major elements while excluding Dy and Pr (as shown in Table 2.2).

Table 2.2 A typical composition of the neodymium iron boron permanent (NdFeB) magnet (Balaram, 2023)

NdFeB-Elements	**Weight percentage %**
Niobium (Nb)	0.5-1.0
Dysprosium (Dy)	0.8-1.2
Boron (B)	1.0-1.2
Neodymium and Praseodymium (NdPr)	29-32
Iron (Fe)	64.2-68.5

Automation, electrification, clean energy, and electronics are vastly dependant on the REE based permanent magnets, especially the elements (Dy, Sm Tb, and Nd), across the consumer, manufacturing, defence, and power generation sectors for having more coercivity The NdFeB continues to be the strongest commercially available permanent magnet because they possess higher energy (about 2.5 times greater) when compared to the samarium cobalt (Sm-Co) magnet. The rare earth Dy provides improved coercivity at high temperature to miniaturize high capacity since these magnets have stronger magnetic fields.

Depending on the end use, the specifications for REE mineral concentrate, metals, and compounds. REEs were traded in various forms since their discovery in the 1970s with mineral concentrates exported, a shift came in the 1980s with REE chemicals such as chlorides and carbonates dominated the markets. Separated REO and metals were in greater demand, followed by REE magnets, phosphors, and polishing powders in the 1990s. REE magnets, computer hard drives, liquid crystal display (LCD), and electric motors took over the markets in the 2000s (Balaram, 2019).

2.13 The applications of rare earths elements (REEs) in modern technology

The zinc cadmium sulphide has been replaced by europium oxide (Eu_2O_3) combined with yttrium oxide (Y_2O_3) in the television industry as they produce brighter coloured pictures on TV screens. The use of REEs extends to phosphor applications such as TV plasma displays and fluorescent lightings as they consume about 90% of europium and terbium, including other elements such as yttrium, gadolinium, cerium, and lanthanum owing to their excellent colour display (Kumari et al., 2015).

The important role of rare earths in military application is acknowledged as well because of their exceptional magnetic strength, which enable

significant component downsizing. REEs are utilized in a variety of applications, including precision guided weapons, space-based satellites, smart bombs, fighter jet engines, night vision goggles, missile guidance systems, coatings and communication systems. Applications in medicine include nuclear medications, portable X-ray devices, magnetic resonance imaging (MRI x-ray tubes), and lasers (dental, medicinal, and surgical). The enhanced MRI apparatus produces a strong magnetic field by employing Dy and Tb in permanent magnets (Kumari et al., 2015).The known applications of REEs are listed in Table 2.3.

Table 2.3 Listing the Applications of rare earth elements (Jepson, 2012; Kumari et al., 2015)

Elements	**Application**
Lanthanum	Ceramics, high optical glasses, glazes, camera lenses, ceramic capacitors, microwave crystals, petroleum cracking, microwave crystals.
Cerium	Cracking catalysts for petroleum, glass polishing, in steel and magnesium (Mg) for improved strength and heat, shielding of radiation, sparking lighters and flints made of ferro-cerium.
Praesodymium	Capacitors made from ceramic, combined with (Nd) for goggles to protect glass makers from sodium glare, cryogenic refrigement, yellow ceramic pigments.
Neodymium	Permanent magnets with superior strength as NdFeB alloy, ceramic capacitors, petroleum cracking, glazes, and coloured glass. (Nd) combined with (Pr) for sodium glare protection.
Promethium	Guided missiles, in harsh environments, radioactive, (Pr) in batteries to power watches.
Samarium	Glass lasers, high magnetic ferro-alloys for as Sm-Co alloy, reactor control and neutron shielding.
Europium	Coloured lamps, red phosphor in nuclear shielding, cathode ray tubes, control rods in nuclear reactor.
Gadolinium	Computer memory chips constituents, cryogenic refrigerants, solid state lasers, high temperature refractories.
Terbium	Computer memories for optical, future hard disk drive, magnets, cathode ray tubes, magneto strictive alloys.
Dysprosium	Alloyed with (Nd) for permanent magnets, catalysts.
Holmium	Refractors, catalysts, controls nuclear reactors.

Erbium	Produce a pink glaze in ceramics, the infra-red absorbing glasses.
Thulium	X–ray source in X-ray machines.
Ytterbium	Practical application presently unknown.
Lutetium	Rechargeable batteries, medical uses, deoxidiser in stainless steel production, superconductors, red phosphor for colour television.
Yttrium	Rechargeable batteries, medical uses, red phosphor for colour television, superconductors, deoxidiser in stainless steel production.
Scandium	Hardened Ni-Cr super-alloys, dental porcelain, x-ray tubes.

As aforementioned, the rapid rise of the REEs application in modern technology has undeniably put a strain on existing rare earths supply chain with experts warning of the supply disruption that may eventually affect the pace of innovation. Hence it is critical for countries of the world over to prioritize research in recycling electronics that have reached the end of life, secure new reserves, and even find substitution for these energy critical materials.

2.14 The productions and trade of rare earth elements

From 1960-85, Mountain Pass mine in California was the world's largest REE producer. By mid 1980s, China became dominant producing 85% of the world 's REE supply accounting for 95% of processed REEs. By 2010s nearly 85% of the world's REE supply was produced by China, while suppling 95% of the processed REEs. The global dominance of China in REEs production is due to its advanced separation and purification technologies, despite uneven resources, consumption, and processing activities worldwide (Bradley et al., 2020).

According to analysis by the U.S Geological Surveys (2022), around 44 metric tons of REOs are lying dormant in Chinese soil, Vietnam as the second largest pile at 22 metric tons, and more than 20 metric tons is believed to lying in the Russian and Brazilian soils. About 61% of the global mine production is done by China, thus mining by far the largest share of the elements traded on the world market. The United States (USA), while the second largest has relatively small market of around 15.5%. Currently REEs are not mined anywhere in Europe with estimated 98% of REEs used in the EU in 2021 imported from China (Armstrong, 2023). From the discussions above, REEs are a vital part of our lives in the 21st century which is technology driven. The application includes laptops computers, mobiles phones

.

CHAPTER THREE: METHODOLOGY AND EXPERIMENTAL

The objective of this chapter is to outline and provide a comprehensive discussion of the materials and methods employed for the subsequent achievements of the specified aims and objectives. The detailed description of procedures, methods, and data collection are included. This section serves as a foundation for providing insight into how the study was conducted and how data was collected.

The methodologies applied in this chapter are illustrated in Figure 3.1 which include the sample preparation, sample decompositions methods, sample analysis, and discussions of the results.

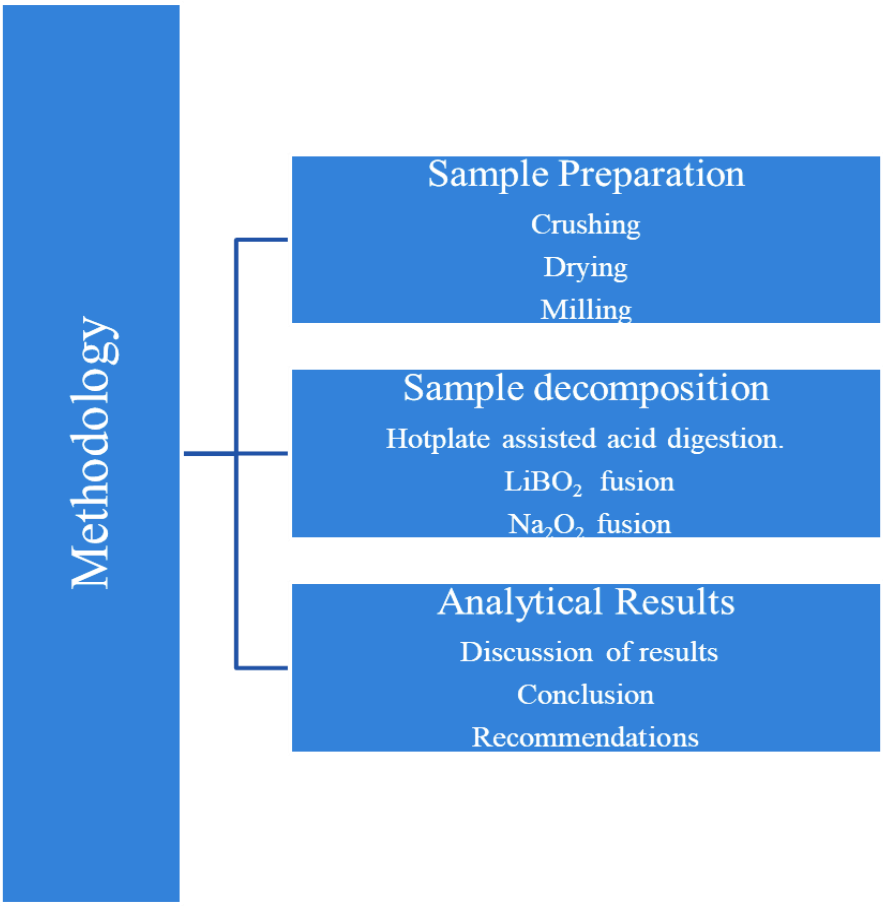

Figure 3.1 A flow of processes in the preparation and analysis of monazite sample

3.1 Materials and calibration standard standards used for experimental

Type 1, Milli-Q system (Merck) was used to prepare the (18.2 M Ω cm) ultrapure water used throughout the study. The analytical grade, ISO grade Acids: hydrochloric acid 37% (w/w), hydrofluoric acid 48% (w/w), Nitric acid 65% (w/w), perchloric acid 70% sourced from (Merck). Johannesburg,

South Africa used during multi acids digestions process. Sodium peroxide (Na_2O_2, 95.00%), sodium hydroxide (NaOH, 97.00%), and tartaric acid used for peroxide fusion were all supplied by (African Chemical enterprise, (ACE), Johannesburg, South Africa while Lithium meta-borate ($LiBO_2$. 95.99%), di-Boron trioxide (B_2O_3 99.99%), and lithium nitrate ($LiNO_3$, 99.995%) used in lithium metaborate fusion were all supplied by Merck, Johannesburg, South Africa. A list of the 1000mg/L of ICP-grade single element Accu Standards were sourced from Stargate (Johannesburg, South Africa) containing the following elements, La, Ce, Pr, Nd, Sm, Eu, Gd, Tb, Dy, Ho, Er, Tm, Yb, Lu, Re, and Nd. The certified reference materials (CRMs) are both radioactive phosphate monazite ore, Institute of Geological Science (IGS-36), and South African Reference Materials (SARM 148) sourced from Richards Bay Minerals, South Africa. The monazite sample from Zandkopsdrift (ZKD) was sourced from the Pyrometallurgical Division of Mintek.

3.2 Experimental

3.2.1. Sample dissolution using open vessel-hotplate assisted digestion method

The method was adopted from literature (Cherviakouski et al., 2024) (Ardini et al., 2010) with slight changes. Approximately 0.2 g of CRM and samples were weighed into 250 mL Teflon beakers (illustrated in the enclosed Figure 10), and about 2 mL of water was used to wash the samples off the walls of the Teflon beakers. Followed by 9 mL of HNO_3 acid, 3 mL $HClO_4$, and 10 mL HF. The beakers were then placed on the hotplate and allowed to digest completely to complete dryness at the temperature of 180ºC ±20. The acid digestion step was repeated with the same amounts of acids to obtain complete dissolution of the refractory minerals. The samples were allowed to cool off, the residue was dissolved into 10 mL 5% HNO_3 acid solution and transferred unto 100 mL flask.

The conventional hot plate assisted-acid digestion procedure depicted in the Figure 3.2, the acid digestion is dependent on the boiling points of the mineral acids used. The heat going into the reaction mixture by convention current comes from the outside of the vessel, resulting in extremely hot Teflon beaker walls.

Figure 3.2 Hotplate assisted acid digestion using Teflon beakers

3.2.2. Sample dissolution using Na_2O_2/NaOH flux fusion method

The method was adapted from literature (Yadav et al., 2012) with minor modification**.** Approximately 0.2 g of CRM and samples directly weighed into 35 mL zirconium crucible, followed by 2 g of granulated Na_2O_2 and two pellets of NaOH and mixed thoroughly. Crucibles were then placed on the Nieka automated fusion machine as securely a glass sash (as illustrated in Figure 3.3). Fusion program lasted for 3 minutes and 10 seconds, wherein the flame increased gradually. A clear red melt attained was allowed to cool before leaching the sample digest into 10mL 5% HNO_3 and transferring into 100 mL glass flask.

Figure 3.3 The sodium peroxide/ sodium hydroxide fusion in progress for the sample decomposition of the sample

Table 3.1 Nieka G8 Peroxide-fluxer machine performance parameters

Parameter	**Conditions**
Gas line	Natural gas
Operation time	3 minutes 30 seconds
Gas power	15 W (Watts)
Rotation speed	15 rpm (rotation per minute)

3.2.3. Sample dissolution using $LiBO_2$ flux fusion method

Approximately 0.2 g of CRM samples were directly weighed into 95% platinum~5% Au crucible. A mixture of flux comprising of 1.5 g $LiBO_2$, 0,8 g of B_2O_3 and 0.3 g $LiNO_3$ was combined thoroughly with the sample. The Pt crucibles and moulds were placed on the automated fusion machine and secured as illustrated in Figure 3.4. Followed by fusion at the temperature of 1050 °C for 20 minutes using a pre heated oven of the automated fusion machine (as seen in Figure 3.5). A homogenous red-hot melt is cast into a 95% platinum-5% Au mold to form a glass bead (as illustrated in Figure 3.6). The glass bead dissolved in 15 mL of HNO_3 and 10 mL HF and allowed to

digest to incipient dryness on the hotplate. The resulting residue dissolved into 10mL 5% of HNO_3 and transferred into 100 mL flask.

Figure 3 4 Mixture of samples and $LiBO_2$ flux placed on six position fusion machines

Figure 3.5 Samples placed in a pre-heated oven for efficient $LiBO_2$ fusion

Figure 3.6 The completed cycle of $LiBO_2$ fusion with the homogenous melt casted on Pt mould

3.3 Instrumentation

3.3.1 Inductively coupled plasma-mass spectrometry (ICP-MS) instrument used for the measuring REEs in solution samples

The REEs concentration in solution samples was measured using inductively coupled plasma -MS (Perkin Elmer 300Q NexION) with the condition stated in the table. The warm-up of the instrument was initiated, followed by daily Instrument performance test for monitoring the instrument sensitivity using the Indium (In) isotope (^{115} In.>30000 counts per second). Using a 1ppb set-up standard, the levels of oxides were monitored by controlling ^{156}CeO <0.5%. The instrument was considered ready for the REEs determination after the daily performance test was successful.

Conducting the daily performance was exceptionally critical in minimizing oxide/ hydroxide interferences, or keeping them at insignificant levels during the REEs determination by ICP-MS (Longerich et al., 1990). Figures 3.7 and 3.8 show the ICP-MS instrument used to measure the REEs, where the

standard (STD) mode and kinetic energy discrimination (KED) mode were optimized. KED mode operates with helium (He) as the carrier gas, and STD mode utilizes argon (Ar) as the carrier gas. The performance parameters of the ICP-MS instrument are listed in Table 3.2.

Figure 3.7 Inductively coupled plasma mass spectrometry (ICP-MS) Perkin Elmer 300Q NexION

Table 3.2 Inductively coupled plasma mass spectrometry (ICP-MS) Perkin Elmer NeXion operating and measurement conditions in KED mode for the REE determinations

Parameter	**Actual Value**
Nebulizer gas flow	0.82 L/min
Auxilliary gas flow	1.3 L/min
Plasma gas flow	15 L/min
RF Power	1300W
Analog pulse voltage	-2331 V
Pulse stage voltage	1000 V
Double charge: Ce++/Ce+	≤ 0.03
Oxide levels; CeO+/Ce+	≤2.5 %
Internal STDs	187 Re and 115 In
Sampler and skimmer cones	Nickel
Number of replicates	3

A series of 1000 ppm single element stock solutions were diluted to prepare a mixed 1 ppm multi-element standard. From the 1 ppm, then working standard solutions containing 5, 10, 20 40, 50, and 100 ppb respectively of each element were prepared by successive dilutions and made in 2% of HNO_3. Working standards, procedural blanks, and samples were spiked with a constant amount of 0.01 ppb of Rhenium (Re) and indium (In) as internal standards to correct for non-spectral interferences, and using a standard mathematical equation, the software corrected for isobaric interferences, as shown in the Table 3.3.

Table 3.3 ICP-MS analysis with potential spectroscopic interferences on selected REEs isotopes

Analyte (*)	**Mass (amu)**	**Corrections**	**Potential interferences**
Sc	44.9559		BO_2, CaH, SiO, CO_2, AlO, Zr
Y	88.9054		
In	114.904	-0.014038 *Sn 118	Sn, MoO
La	138.906		
Ce	139.905		
Pr	140.907		
Nd	145.913		BaO
Sm	146.915		
Eu	150.92		BaO
Tb	158.925		NdO, PrO
Gd	159.927	-0.093976* Dy 163	Dy, NdO, CeO, SmO
Dy	162.925		SmO, NdO
Ho	164.93		SmO
Er	166.932		EuO, SmO
Tm	168.934		EuO
Yb	173.939	-0.005865 * Hf 178	Hf, GdO, DyO
Lu	174.941		GdO, TbO
Re	186.956	-0.121362 * Os 189	Os, YbO, TmO

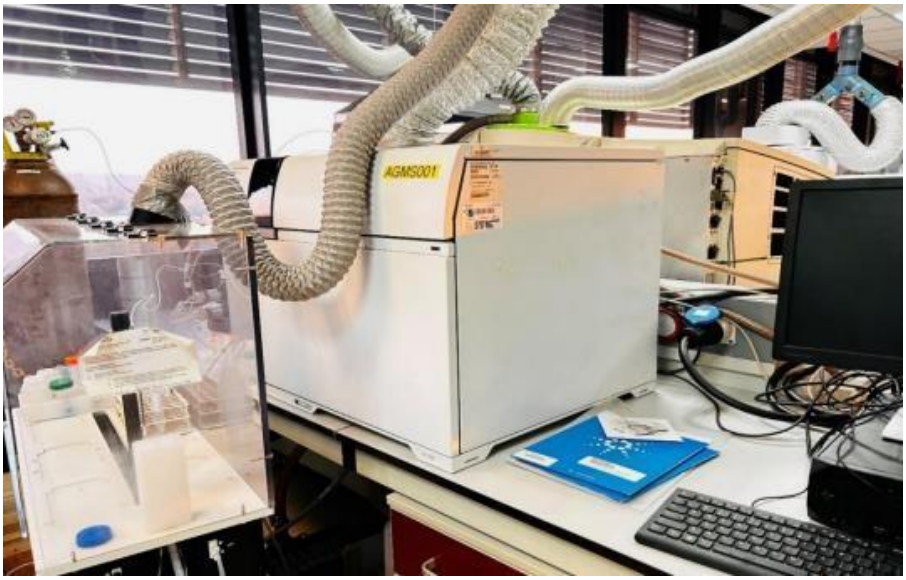

Figure 3.8 Inductively coupled plasma mass spectrometry (ICP-MS) Agilent ICP–MS 7800 instruments

3.3.2 Inductively coupled plasma optical emission spectroscopy instrument (ICP-OES)

An Agilent 5900 ICP–OES (Agilent Technologies Inc., California, United States of America) furnished with the ICP-Expert software (version: 7.5.4.11997). The built-in feature of this Agilent instrument synchronous vertical dual view (SVDS) can capture the plasma's axial and radial views in a single readout. The integrated Advanced Valve System (AVS) maintains the highest level of analytical precision while accelerating the analysis and reduced argon gas consumption. The IntelliQuant smart software collects information across the full wavelength range, detecting spectral interferences, and providing suggestions. Fitted with smart tools such as Fast Automated Curve Fitting (FACT), Fitted Background Correction (FBC), and Inter Element Correct (IEC).

For the REEs analysis, the high purity argon gas employed as both a carrier gas source and a plasma. Selection of the wavelengths was based upon the intrinsic strength and reduced spectral interferences. On-line internal standard solution comprising of Re and In were selected for drift correction.

Advancement of analytical techniques as depicted in Figure 3.9 show how smaller the modern spectrometry has become, and the performance parameters of ICP-OES is listed in Table 3.8. Analysis was performed in radial mode for the REEs, with argon of superior purity utilized as the carrier gas and plasma.

Figure 3.9 Inductively coupled plasma optical emission spectroscopy Agilent 5900 instrument for analysis of REEs

Table 3.4 Performance parameters of the ICP-OES Agilent 5900 instrument

Parameters	**Conditions**
Plasma power	1400 kW
Plasma gas	Argon
Plasma gas flow rate	17 L/min^{-1}
Auxiliary flow rate	1.4 L/min^{1}
Nebulizer gas flow rate	0.85 L/min
Sample uptake rate	1.5 mL/min
Acquisition time	100 seconds
Washout time	120 seconds
Number of replicates	3

3.3.3 Determination of LOD and LOQ

The most prevalent isotope of each element was used to calculate the amount of the analyte that produced a signal equal to three (LOD) and ten times (LOQ) the background standard deviation respectively listed in Table 4.1. The established LODs and LOQs showed how reliable and dependable the ICP-MS technique is for the quantification of REEs.

$$\text{LOD} = 3\times \frac{\text{standard calibration error } (S\frac{y}{x})}{Slope\ (x\ variable)} \qquad \text{equation (1)}$$

$$\text{LOQ} = 10\times \frac{\text{standard calibration error } (S\frac{y}{x})}{Slope\ (x\ variable)} \qquad \text{equation (2)}$$

3.3.4 Repeatability and Reproducibility

The degree of consistency between results while all other factors remain constant is known as repeatability. The consistency in repeatability includes, same instruments, reagents, equipment, used over a brief duration with different analysts. This performance parameter is best demonstrated with the standard deviation (RSD) of replicates generated simultaneously as shown in Table 4.2. The RSD less than 5% and the recoveries within the acceptable limit of 95-100% were achieved by analysing the 10-ppb calibration standard, amounting to ten replicates. Equation 3 shows the calculated RSD wherein the standard deviation (SD) was based on four replicates

$$\text{RSD (\%)} = \frac{SD}{Mean} \times 100\% \qquad \text{equation (3)}$$

The total percent recovery was calculated using equation 4

$$\text{Recovery (\%)} = \frac{x}{x_{ref}} \times 100\% \qquad \text{equation (4)}$$

Where x is the mean concentration of the analyte, x_{ref} is the reference value of the analyte from the certified reference materials.

3.3.5 Statistical methodology for dissolution and qualification of REEs in monazite

The statistical methodology was carried out using the ANOVA (Analysis of Variance) using the Microsoft Excel (the spreadsheet) in data analysis ToolPak. This statistical method is a strong for determining whether there are significant variations in averages across various types of methodologies (or groups). In this study, we compare dissolution methods with ICP-OES (Inductively Coupled Plasma Optical Emission Spectroscopy) and inductively Coupled Plasma Mass Spectroscopy (ICP-MS) analysis. ANOVA can help assess whether different sample preparation techniques like acid digestion, fusion, and microwave-assisted digestion affect the analytical results.

CHAPTER FOUR: RESULTS AND DISCUSSIONS

This aims to discuss the results of the objectives. These includes optimizing conditions for the sample preparation methods used for the monazite as well as those of the analytical techniques. Three sample preparation methods (peroxide fusion, lithium borate, as well as open vessel-hot plate assisted acid digestion). The samples were analysed using both ICP-OES and ICP-MS for the detection of rare earth elements within the solution samples. Some method performance parameters will be discussed.

4.1 Observations from sample dissolution methods

Jarvis and co-workers emphasised on the importance of making a clear distinction during chemical analysis between constraints imposed by either the analytical technique, sample preparation procedure or instrument (Jarvis and Jarvis, 1992). By employing three different sample dissolution techniques showed the importance of selecting a proper and suitable procedure during REEs determination, to suit the sample chemical composition and ultimately the analytes. Elemental analysis using the inductively coupled plasma analytical techniques ICP-OES, and ICP-MS. Each method was evaluated, and comparison was made based on the performance merits such total liberation of REEs from the samples, stability of the resultant solution, ease of use, and cost effectiveness.

4.1.1 The outcome of sample dissolution using sodium peroxide (Na_2O_2/ NaOH) fusion

Few literatures exist on the use sodium peroxide fusion/sintering for the digestion of monazite samples and analysis by ICP-MS, however both fluorides and phosphate fluxes have been reported quite frequently. This study adopted process by Mnculwane (2022) for dissolution of various geological CRMs using high temperature alkaline fusion for quantifying REEs using the ICP-MS. The study involved the fusion of samples in a pre-heated furnace for 45 minutes at temperature of 600 °C. Bokhari (2016) studied and compared various sample to flux ratios, the sample to flux ration of 1:6 was suggested to be more effective for complete dissolution of zircon bearing mineral for a duration of 120 minutes. However, for this study, the sample to flux ration of 1:10 was used since monazite contains associated refractory mineral such as rutile, zircon, ilmenite and, quartz.

Various authors have employed peroxide fusion /sintering by muffle furnace at the temperatures ranging from 480-520 °C, with contact time varying between 30 minutes to 2 hours. In this study, auto-fusion machine with open flame consisting of natural gas, and compressed air was used which was instrumental in ensuring total sample dissolution in less than five minutes with the temperature as high as 480 °C reached within seconds(Bokhari & Meisel, 2017; Mnculwane, 2022b)..

Total sample dissolution was observed with the sinter cake from a flux mixture of sodium peroxide (Na_2O_2) and sodium hydroxide (NaOH) that readily dissolved in water as observed by other authors including Bokhari (2016). The short fusion duration may be attributed to the increased strength of the flux mixture of two oxidizing agents (Na_2O_2 and NaOH) as well as the source of heat comprising of combination of natural gas and compressed air flame. Furthermore, the reaction of Na_2O_2 with water generates NaOH which precipitates the REEs as rare earth hydroxides (Chao and Sanzolone., 1992).

Also, adding two pellets of NaOH during fusion might have further increased the recoveries of REEs. However, it also increased the sodium content in the solution matrix which may have impacted the plasma and the ICP-OES's sensitivity. The literature studies have indicated that sodium ion has a negative influence on the ICP-OES properties which may enhance the analyte intensities (Xaba et al., 2018a) . Prior to analysis of digest samples in Na_2O_2 matrix, further dilutions were made to reduce total dissolved solids (TDS). The use of Na_2O_2 for the dissolution of monazite followed by ICP-MS method was found to be easy, rapid, cost-effective and best suited for refractory minerals while providing higher samples throughput. Zirconium crucibles were used for this study, although they are not as durable as the Pt crucibles, they are best suited for sodium peroxide fusion or sintering as compared to nickel crucibles which get easily corroded by the flux (Mnculwane, 2022a).

.

4.1.2 The outcome of sample dissolution using lithium metaborate ($LiBO_2$) fusion

Fusion using mixture of $LiBO_2/Li_2B_4O_7$ was also employed for this study due to its capability of destruction of refractory minerals during chemical analysis of REEs in geological and metallurgical samples. According to Chao (1992) $LiBO_2$ can be substituted with an equivalent amount molar combination of lithium carbonate (Li_2CO_3) and di-boron trioxide (B_2O_3). During fusion excess $LiBO_2$ is generated for the effective decomposition of sample (Chao., 1992). The fusion procedure using lithium metaborate flux at the temperature of 1050 °C for 15 minutes was found to be highly effective resulting in a homogenous glass bead suitable for dissolution in acids prior to liberate REEs in solution for accurate determination. Complete sample dissolution was achieved, however the viscosity resulting from large quantities of silica and boron caused blockage to sample introduction system during samples analysis, affecting the sensitivity of the ICP-MS.

Treating the resulting melt with HF/HNO_3 mixture removed the Si and B as volatile silica tetrafluoride (SiF_4) and tetrafluoroboric acid (HBF_4) as suggested thus liberating the HREEs from Zircon (SiO_2) mineral (Panteeva et al., 2003). The ability of lithium metaborate flux fusion for complete sample dissolution and the ease of use of the automatic fluxer machine was also observed and reported in previous studies Makombe et al, (2017). In this study lithium nitrate ($LiNO_3$) was used instead of Li_2CO_3 for the generation of excess $LiBO_2$. The dissolution method is suitable for the accessory minerals such as monazite, zircon, rutile and others found in the CRMs used in this study. The final solution contained minimal TDS and

viscosity rendering it suitable for ICP-MS analysis. The flux mixture was not corrosive towards platinum (Pt) crucible, though the crucible is found to be most durable, the disadvantage is that they do not come cheap and as precious metals. The suggested method in this study is recommended for REEs analysis in monazite and associated minerals as it may be profitable.

4.1.3 The outcome of sample dissolution using hotplate assisted multi acids digestion

The effectiveness of the popular yet simple open vessel multi acids digestion was explored using the combination of $HF/HNO_3/HClO_4$ in this study. Padmasubashini et al., (2022) repeated the sulphuric fuming steps for monazite resulting in complete digestion of refractory minerals, the same concept was applied in this study where the acids mixture was added repeatedly to ensure sufficient sample dissolution of refractory minerals (Padmasubashini et al., 2022). The flexibility in controlling the addition of reagents and digestion parameters like temperature and time was realised to achieve sample dissolution (Matusiewicz, 2003).

Although the method provided partial sample dissolution, recoveries from ICP-MS indicated that REEs were completely liberated from the matrix sample. The method of multi acids digestions followed by ICP-MS determination of REEs proved to be successful, implying that the dissolution procedure can be employed interchangeably with alkaline fusion using either lithium metaborate or peroxide fusion for REEs determination in monazite. The method was easy to follow, with low procedural, however the drawback is the number of reagents used as well as prolonged digestion time Another challenge was unevenly distributed heat on the hotplate during sample digestion, the use of silica sand on the hotplate resultant in the evenly spread heat on the hotplate. Teflon beakers used in acid digestion are durable, suited for HF use and cost effective.

4.2 Elemental characterization of REEs by inductively coupled plasma

Elemental analysis is a crucial step during the REEs measurements, and by understanding the difference in the application and suitability of each techniques provides an informed decision in selection of the most suitable technique for the specific application. Interference management, detection limit, elemental range, and sample throughput were some of the aspects given attention in this study. The elemental analysis of REEs using both ICP-MS and ICP-OES are discussed. In terms of principles, the ICP-MS directly measures the elements as ions using the mass spectrometer while the ICP-OES measures the light as is emitted from elements using optical spectrometer. For the resolution of spectral overlaps by interfering ions, collision reaction cell (CRC) mode involving helium (He) gas was applied for removal of polyatomic ions on multiple analyte masses.

Several authors including have discussed the spectral interferences from both minor and major elements which may have direct effect on the accurate determinations of REEs by ICP-OES, for which cation-ion separation procedure is often recommended. The presence of high concentration matrix elements at the range of 500-1000 ppm, especially heavy matrix elements such sodium (Na) and uranium (U) may cause signification suppression or enhancement of analyte (Jarvis and Jarvis, 1992). The high concentration levels of REEs and Th in monazite results in abnormal background radiation and reduced emission signals intensities(Jarvis & Jarvis, 1992b)(Rucandio, 1992).

According to literature, the solution sample aspirated directly has significant amounts of Nd, La, Pr, and Ce which caused severe spectrum interference during the ICP-OES analysis of Eu, Gd, Tb, Er, and Tm in monazite matrix.

The analyte spectra were frequently obscured by the wing and direct overlap (Premadas and Khorge, 2006). Based on the line-rich spectra of REEs, the emission intensity decreases with increasing matrix concentration. As background intensities increase, the net intensities decreases (Rucandio, 1992). Elimination or minimization of interfering elements is required for reliable and accurate REEs results using emission spectroscopy.

4.2 Comparison of ICP-OES and ICP-MS based on the dissolution methods

Three different methods of sample dissolution were assessed for this study with the aim to obtain homogenous sample solution suitable for analysis using both the ICP-OES and ICP-MS analytical techniques for the accurate characterization of REEs in the monazite samples. The individual concentrations of the REEs in the monazite samples were measured using both ICP-MS and ICP-OES. The daily instrument performance check as well as calibration were performed prior to sample analysis to ensure the adequate performance and sensitivity of the instrument to detect the elements of interest. The regression plot obtained for all the REEs range R^2=0.999-1.0.

Table 4.1 shows the limits of detection (LOD) and quantification (LOQ) for determining Rare Earth Elements (REEs) using ICP-MS. The blank intensities and calibration coefficients (R^2) range from 0.9990 to 1.0000, demonstrating high calibration accuracy. The LOD values are extremely low, illustrating the method's sensitivity, with the lowest values recorded for components such as Yb (0.00006 ppm) and Lu (0.00004 ppm). The LOQ values are also low, demonstrating the method's capacity to accurately measure REEs at trace quantities, making it ideal for precise investigation of these elements in a variety of samples.

Table 4.1 The LODs and LOQs for the REEs determination on ICP-MS

Blank Intensities	**R^2**	**LOD /ppm**	**LOQ /ppm**
^{89} Y	0.9993	0.00279	0.00932
^{139} La	0.9996	0.00881	0.02899
^{140} Ce	0.9995	0.01559	0.05208
^{141} Pr	0.9995	0.00602	0.02053
^{146} Nd	0.99910	0.00099	0.00309
^{147} Sm	0.99990	0.00021	0.00069
^{153} Eu	0.99900	0.00027	0.00071
^{157} Gd	0.99920	0.00130	0.00441
^{159} Tb	0.99990	0.00053	0.00080
^{163} Dy	1.00000	0.00056	0.00010
^{165} Ho	0.99950	0.00010	0.00063
^{166} Er	0.99970	0.00022	0.00084
^{172} Yb	0.99990	0.00006	0.00014
^{169} Tm	0.99990	0.00019	0.00063
^{175} Lu	1.00000	0.00004	0.00010

Table 4.2, evaluates the stability and repeatability of rare earth elements (REEs) in a quality control (QC) sample, with an emphasis on precision and recovery. The average concentrations of REEs are near to predicted levels, with most elements showing recoveries of 90% to 99%. This shows that the analytical process is effective and that the REEs are accurately measured. The standard deviation (SD) numbers are relatively low, indicating minimal fluctuation in the measurements, and the relative standard deviation (RSD) percentages are likewise low, highlighting the data's high precision. Most elements have RSD values considerably below 1%, indicating remarkable repeatability and consistency over many measurements. Nevertheless, a

few REEs have slightly higher fluctuation. For example, neodymium (Nd) has the highest RSD in the dataset at 1.47%, indicating an irregularity or interference in measurement. Despite this, the Nd recovery rate remains within an acceptable range of 90%. Similarly, terbium (Tb) has a reduced recovery of 90%, but its RSD remains low, indicating that repeatability is not severely affected. Overall, the data show a well-controlled analytical method with few outliers, indicating strong stability and repeatability for the bulk of the REEs in the QC sample. The findings suggest an effective analysis method that is both dependable and precise for monitoring REEs in a variety of applications.

Table 4.2 Stability and repeatability of REEs evaluated on the QC sample

QC standard	Average(ppm)	Expected (ppm)	SD (ppm)	RSD %	Recovery %
^{89} Y	9.830	10.00	0.057	0.588	98
^{139} La	9.780	10.00	0.038	0.392	92
^{140} Ce	9.810	10.00	0.045	0.0462	98
^{141} Pr	9.830	10 .00	0.025	0.348	98
^{146} Nd	9.030	10.00	0.034	1.470	90
^{147} Sm	9.020	10.00	0.133	0.481	99
^{153} Eu	9.510	10.00	0.043	0.431	95
^{157} Gd	9.610	10.00	0.041	0.0882	96
^{159} Tb	9.640	10.00	0.006	0.453	90
^{163} Dy	9.070	10.00	0.085	0.644	90
^{165} Ho	9.690	10.00	0.041	0.490	95
^{166} Er	9.150	10.00	0.088	0.666	92
^{172} Yb	9.670	10.00	0.047	0.474	90
^{169} Tm	9.890	10.00	0.055	0.552	99
^{175} Lu	9.620	10.00	0.049	0.511	96

4.3 Determining linearity and specificity

The regression plot obtained for all the REEs range R^2=0.999-1.0, as shown in Figure 4.1. The linearity shows the suitability of the method for the analysis of REEs with the value of 0.9995 for Ce.

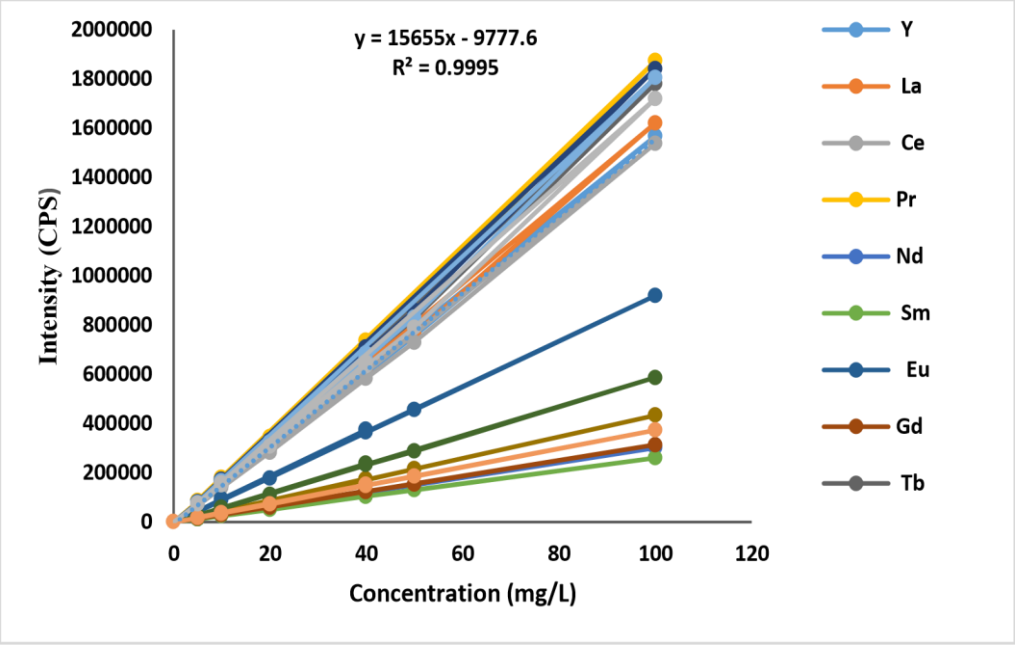

Figure 4.1 Linearity depicted by correlation coefficient (R^2)

CHAPTER FIVE: Characterization and quantification of the heavy and light rare earth elements

This chapter encompasses the elemental characterization of light rare and heavy rare earth in monazite. The concentrations results obtained include those of the optimised sample digestion methods, quantified using ICP-OES and ICP-MS. The obtained analytical data is discussed in the form of graphs and tables.

5.1 Statistical data yielded from characterization of SARM 148 sample fused using Na_2O_2/ NaOH

The results for the SARM 148 that was fused using Na_2O_2/ NaOH, the sample aliquot was taken from the single preparation and analysed using both ICP-OES and ICP-MS are illustrated in Table 5.1 and Figure 5.1. The recovery of rare elements from ICP-MS analysis is in the range of 90-110%, indicating the accuracy and selectivity of the method. Another aliquot from the same sample was measured using ICP-OES, and the recoveries for Yb and Tb, are 44 % and 670% respectively, indicating significant suppression or enhancement on their concentration. The recoveries for Sm and Gd are 92% and 94% respectively, suggesting the elements are not suppressed in this matrix. Recoveries for other elements were below 80%. Therefore, Tb and Yb results indicates the poor reliability and integrity of the ICP-OES technique for REEs determinations. Tb could not be detected from the same solution analysed by ICP-MS attributed to significant suppression from interfering elements.

Table 5.1 Accuracy results for SARM 148 after peroxide Na_2O_2/ NaOH fusion

Element	**SARM148 Certified (ppm)**	**ICP-MS Obtained (ppm)**	**ICP-MS Recoveries %**	**ICP-MS RSD %**	**ICP-OES Obtained (ppm)**	**ICP-OES Recoveries %**	**ICP-OES RSD %**
Y	969 ± 139	976	101	0.5	575	59	36.1
La	11975 ± 458	11638	97	2.0	8672	72	22.6
Ce	22742 ± 1770	21973	97	2.4	15917	70	25.0
Pr	2633 ± 167	2446	93	5.2	1797	68	26.7
Nd	9462 ± 452	9485	100	0.2	7382	78	17.5
Sm	1494 ± 134	1437	96	2.8	1387	92	5.7
Eu	33.1 ± 4.37	31.1	94	4.4	15.8	48	50
Gd	840 ± 45.2	895	107	4.5	787	94	4.6
Tb	93.4 ± 15.6	89.6	96	2.9	n.d	0	0
Dy	282 ± 30.5	274	97	2.0	215	76	19.1
Ho	39.2 ± 3.6	37	94	4.1	29	74	21.2
Er	96.9 ± 16.9	94	97	2.1	60.4	62	32.8

Yb	51.4 ± 4.81	50.7	101	1.0	22.6	44	55
Tm	7.76 ± 1.729	7.07	97	6.6	52	670	105
Lu	7.18 ± 0.796	7.74	108	5.3	4.16	59	37.7

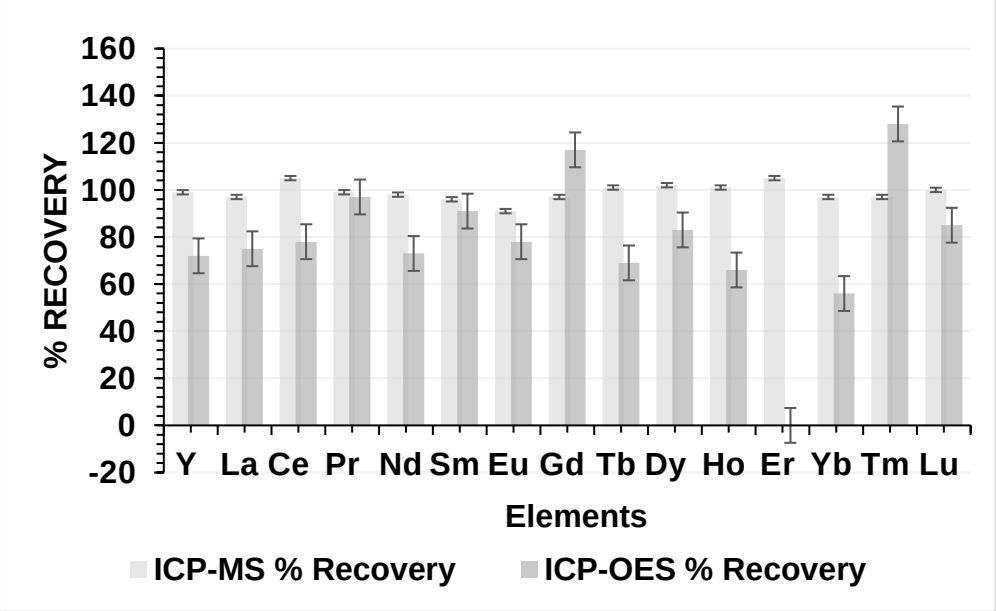

Figure 5.1 REE recoveries for SARM 148 fused using Na_2O_2/ NaOH fusion method

5.2 Statistical data yielded from characterization of SARM 148 sample digested using multi acids hotplate digestion

The results for the CRM SARM 148 sample digested using multi acids hotplate digestion are displayed Table 5.2 and Figure 5.2. Recoveries from ICP-MS analysis is in the range of 90-110% as obtained with peroxide fusion, indicating the accurate and selectivity of the method. Recoveries for LREEs such as La, Ce, Sm, Dy, as well as Y agree well with certified values using ICP-MS. Tb was not detectable while there is over recoveries for Nd, Gd, Er, Ho, Tm and Lu which may be due to interferences. Analytical data by ICP-MS indicated that all the REEs are liberated from the sample.

Table 5.2 Accuracy results for SARM 148 after multi acid digestion

Element	SARM148 Certified (ppm)	ICP-MS Obtained (ppm)	ICP-MS Recoveries %	ICP-MS RSD %	ICP-OES Obtained (ppm)	ICP-OES Recoveries %	ICP-OES RSD %
Y	969 ± 139	919	101	0.5	910	94	4.4
La	11975 ± 458	11530	97	2.0	11676	98	1.8
Ce	22742 ± 1770	22530	97	2.4	23115	102	1.2
Pr	2633 ± 167	2503	93	5.2	2477	94	4.3
Nd	9462 ± 452	9374	100	0.2	12510	132	19.6
Sm	1494 ± 134	1353	96	2.8	1378	92	5.7
Eu	33.1 ± 4.37	34.4	94	4.4	25.6	77	18.1
Gd	840 ± 45.2	826	107	4.5	1297	154	30.2
Tb	93.4 ± 15.6	91	96	2.9	n.d	0	0
Dy	282 ± 30.5	273	97	2.0	284	101	0.5
Ho	39.2 ± 3.6	39.4	94	4.1	68.4	174	38.4
Er	96.9 ± 16.9	97.3	97	2.1	229	236	57.3

Yb	51.4 ± 4.81	52.5	101	1.0	40.4	79	16.9
Tm	7.76 ± 1.729	7.32	97	6.6	52	670	105
Lu	7.18 ± 0.796	7.17	100	5.3	11.6	162	33.3

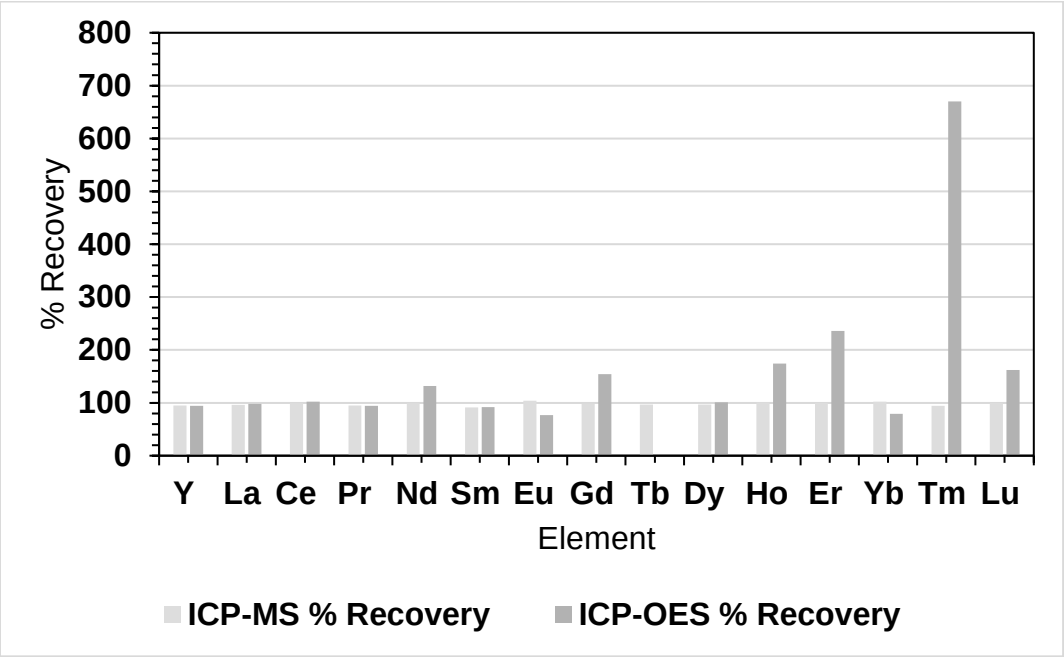

Figure 5.2 REEs recoveries for SARM 148 digested using hotplate multi acid digestion method

5.3 Statistical data yielded from characterization of SARM 148 sample fused using $LiBO_2$ flux

The results for SARM 148 sample fused using $LiBO_2$ method is shown in Table 5.3 and Figure 5.3. Recoveries from ICP-MS analysis is in the range of 90-110% as obtained with peroxide fusion, indicating the accuracy and selectivity of the method. Recoveries for LREEs such as La, Sm, Dy, Pr as well as Y agree well with published data using ICP-OES. The elements that were not detectable were Tb, Eu, and Er while there is over recoveries for Nd, Gd, Er, Ho, Tm and Lu which may be due to interferences. Analytical data by ICP-MS indicated that all the REEs are liberated from the sample.

Table 5.3 Accuracy results for SARM 148 after $LiBO_2$ fusion

Element	**SARM 148 Certified (ppm)**	**ICP-MS Obtained (ppm)**	**ICP-MS Recoveries %**	**ICP-MS RSD %**	**ICP-OES Obtained (ppm)**	**ICP-OES Recoveries %**	**ICP-OES RSD %**
Y	969 ± 139	1024	106	3.9	980	101	0.8
La	11975 ± 458	11140	93	5.1	12624	105	3.7
Ce	22742 ± 1770	22691	100	0.2	13790	61	34.7
Pr	2633 ± 167	2534	96	2.7	2611	99	0.6
Nd	9462 ± 452	9488	100	0.2	12510	132	19.6
Sm	1494 ± 134	1382	93	5.5	1278	86	11.0
Eu	33.1 ± 4.37	32.4	98	1.5	n.d	0	0
Gd	840 ± 45.2	848	101	0.7	1467	175	38.4
Tb	93.4 ± 15.6	93.7	100	0.2	n.d	0	0
Dy	282 ± 30.5	282	102	0.0	303	107	5.1
Ho	39.2 ± 3.6	40.1	99	1.6	29	74	21.2
Er	96.9 ± 16.9	95.8	99	0.8	n.d	0	0

Yb	51.4 ± 4.81	50.2	98	1.7	46.8	91	6.6
Tm	7.76 ± 1.729	7.70	100	0.5	41	528	96.4
Lu	7.18 ± 0.796	7.17	100	0.1	4.19	58	37.2

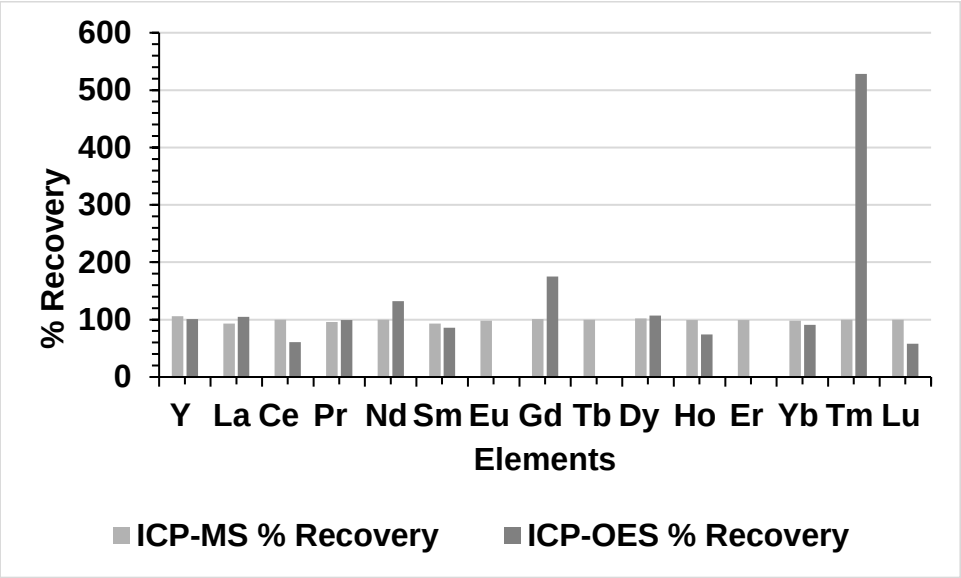

Figure 5.3 REEs recoveries for SARM 148 fused using $LiBO_2$ fusion method

5.4 Statistical data yielded from characterization of IGS-36 sample digested using multi acids hotplate digestion

Table 5.4 and Figure 5.4 show the results for the CRM, IGS-36 sample digested using multi acids hotplate digestion. Recoveries from ICP-MS analysis is in the range of 90-110% as obtained with peroxide fusion, indicating the accurate and selectivity of the method. Recoveries for La, and Sm measured by ICP-OES were found to be lower at 68% range. All the REEs were detectable by ICP-OES, presenting a confusing picture as Tb was undetectable in SARM 148. Analytical data by ICP-MS indicated that all the analytes are liberated from the sample.

Table 5.4 Accuracy results for IGS-36 after multi acid digestion.

Element	IGS-36 Certified (ppm)	ICP-MS Obtained (ppm)	ICP-MS Recoveries %	ICP-MS RSD %	ICP-OES Obtained (ppm)	ICP-OES Recoveries %	ICP-OES RSD %
Y	8800 ± 1870	8294	94	4.2	8017	91	6.6
La	102000 ± 8330	96390	95	4.0	69288	68	27.0
Ce	203000 ± 9250	198730	98	1.5	184266	91	6.8
Pr	23000 ± 1590	21818	95	3.7	21967	96	3.2
Nd	99560 ± 6940	98221	99	1.0	68034	68	26.7
Sm	13300 ± 1910	12938	97	2.0	11253	85	11.8
Eu	301 ± 39	272	90	7.2	204	68	27.7
Gd	6500 ± 350	6238	96	2.9	8454	130	18.5
Tb	1000 ± 530	1058	106	4.0	937	94	4.6
Dy	2700 ± 600	2450	91	6.9	2471	92	6.3
Ho	347 ± 24	355	102	1.6	327	94	4.2
Er	535 ± 19	489	91	6.4	404	76	19.7

Yb	256 ± 39	231	90	7.3	399	156	30.9
Tm	57 ± 16	52.1	90	7.7	67	118	11.4
Lu	51 ± 7	49.3	97	2.4	57	112	7.9

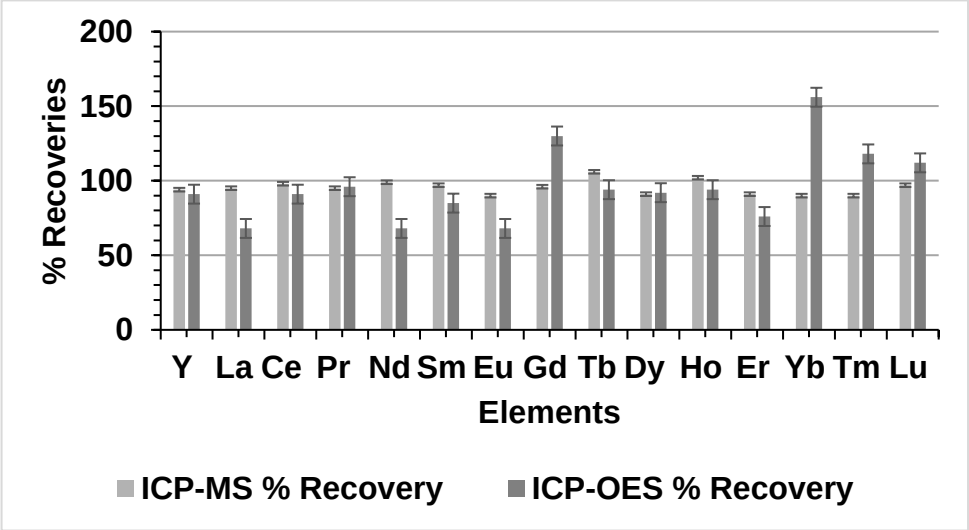

Figure 5.4 REEs recoveries for IGS-36 digested using hotplate assisted multi acids digestion method

5.5 Statistical data yielded from characterization of IGS-36 sample fused using $LiBO_2$ flux

The results for the CRM IGS-36 sample fused using $LiBO_2$, are displayed in Table 5.5 and Figure 5.5. Recoveries from ICP-MS analysis is in the range of 90-110% as obtained with peroxide fusion and multi-acids hotplate digestion, indicating the accurate and selectivity of the method. Recoveries for LREEs such as La, Ce, Sm, Dy, as well as Y agree well with certified values from CRM using ICP-OES. The observation made suggests that $LiBO_2$ fusion coupled with ICP-OES can be used for REE determinations in monazite associated mineral. Elements such asTb was not detectable while there over recoveries for Pr, Gd, Tm and Lu which may be due to interferences was observed. Analytical data by ICP-MS indicated that all the analytes are liberated from the sample and the method is selective and accurate.

Table 5.5 Accuracy results for IGS-36 after $LiBO_2$ fusion

Element	**IGS-36 Certified (ppm)**	**ICP-MS Obtained (ppm)**	**ICP-MS Recoveries %**	**ICP-MS RSD %**	**ICP-OES Obtained (ppm)**	**ICP-OES Recoveries %**	**ICP-OES RSD %**
Y	8800 ± 1870	8785	100	0.1	8080	92	6.0
La	102000 ± 8330	94662	93	5.3	104568	103	1.8
Ce	203000 ± 9250	194940	96	2.9	212619	105	3.3
Pr	23000 ± 1590	22437	98	1.8	28773	125	15.8
Nd	99560 ± 6940	98803	99	0.5	92753	93	5.0
Sm	13300 ± 1910	13436	101	0.7	15630	118	10.5
Eu	301 ± 39	299	99	0.5	284	94	4.1
Gd	6500 ± 350	6843	105	3.6	9643	148	14.2
Tb	1000 ± 530	997	100	0.2	862	86	10.5
Dy	2700 ± 600	2729	101	0.8	2955	109	2.64
Ho	347 ± 24	341	98	1.2	319	92	5.9
Er	535 ± 19	517	97	2.4	n.d	0	0

Yb	256 ± 39	253	99	0.8	282	110	6.8
Tm	57 ± 16	57	100	0.0	83	146	26.3
Lu	51 ± 7	50.8	100	0.3	61.3	120	13.0

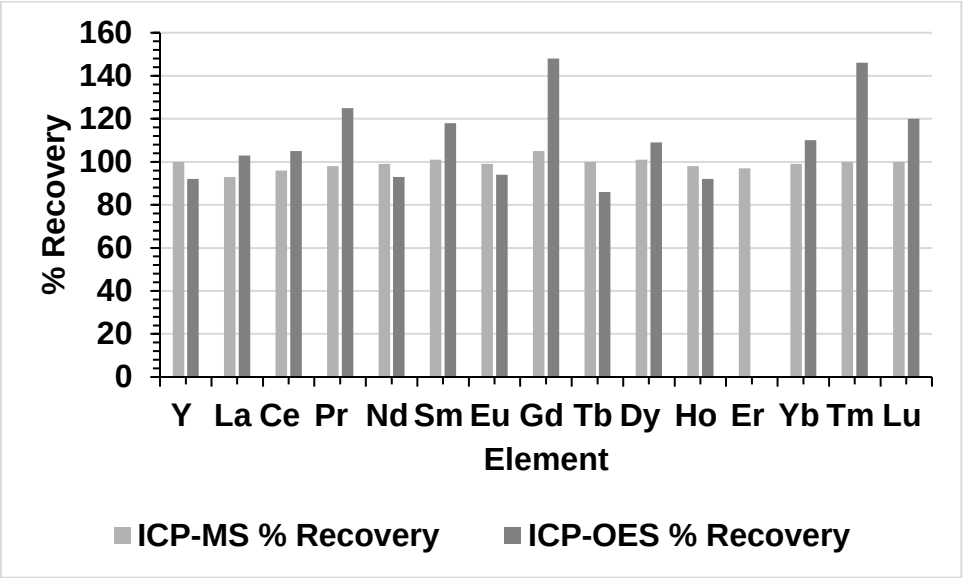

Figure 5.5 REEs recoveries for IGS-36 fused using $LiBO_2$ fusion method

5.6 Statistical data yielded from characterization of IGS-36 sample fused using Na_2O_2/ NaOH

The results for the CRM IGS-36 fused using Na_2O_2/ NaOH is displayed in Table 5.6 and Figure 5.6. The recoveries of rare elements from ICP-MS analysis where in the range of 90-110%, indicating the accuracy and selectivity of the method. However, the analytical data from ICP-OES analysis tells a different story as observed with SARM 148. Er (296.452) and Er (326.478) were not detectable, as the scan indicated other rare earth elements such Ce, Yb, Tb, Nd, and Sm as interferents. Lu at the concentration range of 51% of Ce, and Yb is detectable with recoveries of 85%. There is an anomaly with Tm even at the 57.0 ppm concentration range, the recoveries are over ranging at 128%.

Table 5.6 Accuracy results of REEs for IGS-36 after Na_2O_2/ NaOH fusion

Element	**IGS-36 Certified (ppm)**	**ICP-MS Obtained (ppm)**	**ICP-MS Recoveries %**	**ICP-MS RSD %**	**ICP-OES Obtained (ppm)**	**ICP-OES Recoveries %**	**ICP-OES RSD %**
Y	8800 ± 1870	8723	99	0.6	6328	72	23.1
La	102000 ± 8330	99076	97	2.1	76703	75	20.0
Ce	203000 ± 9250	212158	105	3.1	158608	78	17.4
Pr	23000 ± 1590	22747	99	0.8	22259	97	2.3
Nd	99560 ± 6940	97358	98	1.6	72816	73	21.9
Sm	13300 ± 1910	12738	96	3.1	12109	91	6.6
Eu	301 ± 39	273	91	6.9	235	78	17.4
Gd	6500 ± 350	6321	97	2.0	7611	117	11.1
Tb	1000 ± 530	1009	101	0.6	687	69	26.2
Dy	2700 ± 600	2751	102	1.3	2229	83	13.5
Ho	347 ± 24	352	101	1.0	228	66	29.3
Er	535 ± 19	560	105	3.2	n.d	0	0

Yb	256 ± 39	249	97	2.0	143	56	40.1
Tm	57 ± 16	55.1	97	2.4	73	128	17.4
Lu	51 ± 7	50.8	100	0.3	43.1	85	11.9

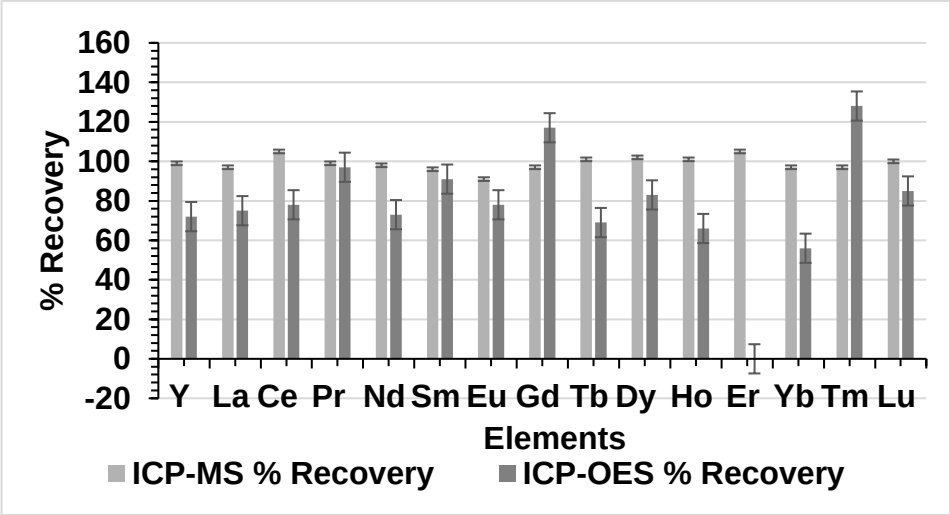

Figure 5.6 REEs recoveries for IGS-36 fused using Na_2O_2/ NaOH fusion method

5.7 Statistical data yielded from characterization of ZKD sample using Na_2O_2/ NaOH, $LiBO_2$, and hotplate multi-acids assisted digestion

Table 5.7 and Figure 5.7 show the analytical data obtained for the ZKD sample prepared using the three methods. The first column (element) shows the selected isotopes REEs determination during the ICP-MS analysis. The second column ($LiBO_2$ fusion) shows data for the lithium metaborate fusion. The third column shows data for sodium peroxide fusion (Na_2O_2/NaOH), and lastly, the fourth column shows data for multi (HT) acids digestion method. For each method, the TREEs were calculated using Horwitz statistical tool, and the variation between these methods was within the variance of 5%. The results below it can be concluded that the methods can be used interchangeably for accurate REEs determination. Rare earth elements in ZKD monazite sample were measured using ICP-MS since the optimal conditions were achievable.

Table 5.7 Elemental analysis results for ZKD sample prepared using $LiBO_2$ fusion, NaOH fusion, and multi acids digestion and analysis by ICP-MS

Element	**$LiBO_2$ fusion (ppm)**	**Na_2O_2/NaOH fusion**	**HT multi-acid digestion**
^{89} Y	864	964	940
^{139} La	6488	6420	6087
^{140} Ce	10622	11760	10670
^{141} Pr	3511	3268	3273
^{146} Nd	1085	1060	1080
^{147} Sm	494	504	518
^{153} Eu	124	122	118
^{157} Gd	345	357	401
^{159} Tb	46.5	47.0	46.4
^{163} Dy	184	181	186
^{165} Ho	29.5	27.4	29.7
^{166} Er	90.9	92	86.3
^{172} Yb	8.41	8.27	7.44
^{169} Tm	57	58.9	54.1
^{175} Lu	7.14	7.12	6.36
TREEs	**23957**	**24877**	**23503**

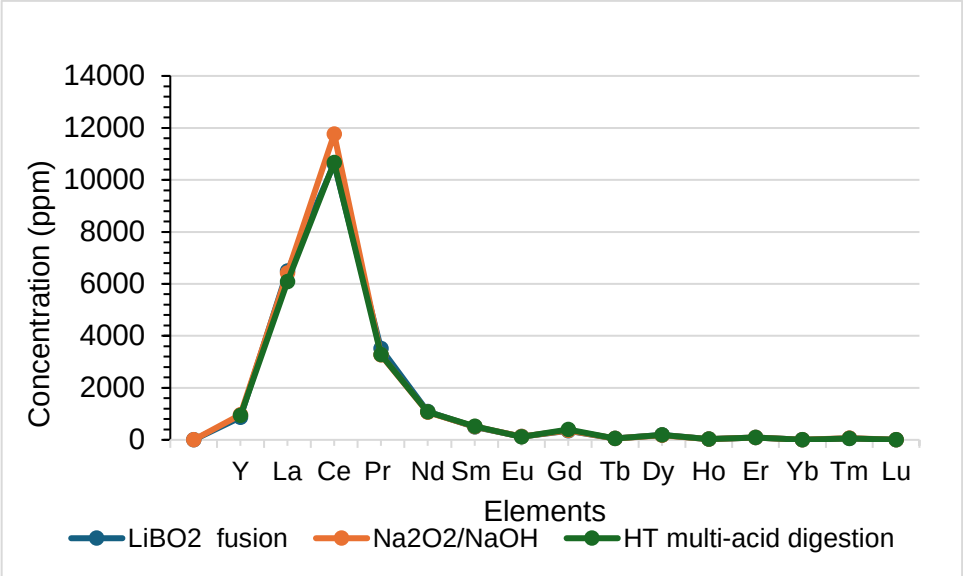

Figure 5.7 Comparison of different sample preparation of the ZKD sample measured by ICP-MS

5.8 Statistical data yielded from characterization of ZKD sample using Na_2O_2/ NaOH, $LiBO_2$, and hotplate multi-acids assisted digestion ICP-OES

Table 5.8 and Figure 5.8 show the analytical data obtained for the ZKD sample prepared using the three methods. In contrast to ICP-MS analysis, there are inconsistent recoveries for all the different techniques. Results for La, Ce, and Lu digested using multi acids digestion compares to the results obtained using ICP-MS. Er was found not to be detected in the $LiBO_2$ and Na_2O_2/ NaOH matrices. It is difficult to make a conclusion as the results do not follow any trend as compared to the ZKD analysed using ICP-MS.

.

Table 5.8 Elemental analysis results for ZKD sample prepared using $LiBO_2$ fusion, NaOH fusion, and multi acids digestion and analysis by ICP-OES

Element	**$LiBO_2$ fusion (ppm)**	**Na_2O_2/NaOH fusion (pp)**	**HT multi-acid digestion (ppm)**
Y	993	364	827
La	11742	4609	6093
Ce	7061	7153	10680
Pr	1216	865	1080
Nd	8464	0	3831
Sm	636	459	543
Eu	139	175	133
Gd	775	460	212
Tb	34.7	30.7	41.2
Dy	235	153	195
Ho	43.3	19.2	48.0
Er	0	0	69.9
Yb	76.2	29.2	58.4
Tm	41.9	52.1	30.7
Lu	3.68	3.94	7.81
TREEs	2097	958	1590

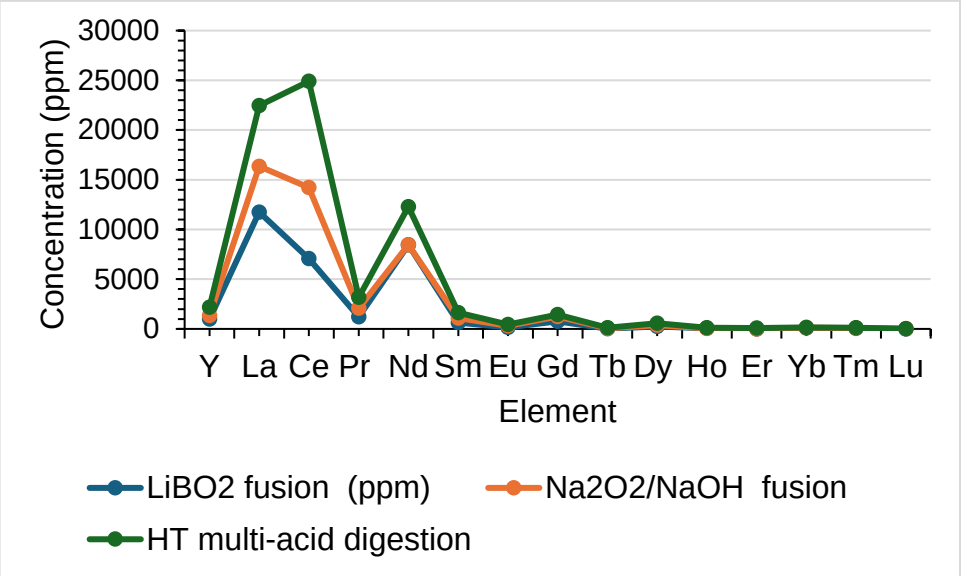

Figure 5.8 Comparison of different sample preparation of the ZKD sample measured by ICP-OES

5.9 The spectra showing the most interfered elements from ICP-OES

Figures 5.9 to 5.12 contains the spectra from the ICP-OES, showing the significantly interfered elements (Tb, Er, Gd, and Tm). In the Figures the green line indicates the analyte, the red dotted line represents the interferences, while the blue line is the combination of both the analyte and the interferences or the background matrix. Tb on both wavelengths is suppressed significantly by sample matrix elements, leading to the analyte been undetectable. Peaks detected for Gd and Tm are those of the background showing significantly elevated results. This observation suggests that matrix separation of REEs from the sample is required. Figure 5.9 shows the spectrum of analyte Tb at wavelength 370.392nm (green line), with the peak not properly defined and spectrally interfered. The Tb recovery for IGS-36 is 69% which is lower than the acceptable recovery ranges of 80-120%, and not detectable for SARM 148 in samples fused in peroxide flux. The recovery for Tb in samples digested in $LiBO_2$ for SARM 148 is not detectable, while the recovery for IGS-36 is 86%.

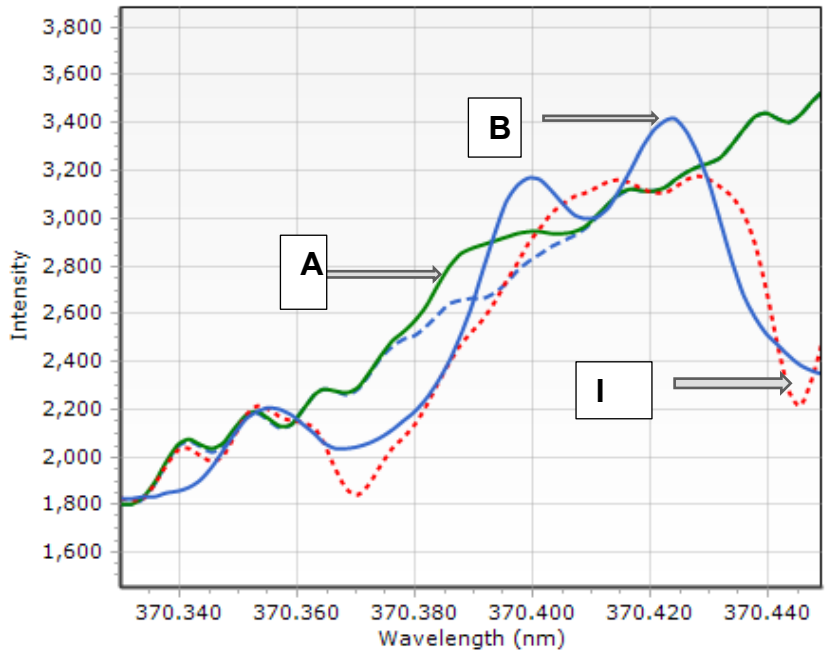

Figure 5.9 ICP-OES Spectrum for Tb at the wavelength (370.392nm), (A=analyte, B=Background matrix , I= interferences)

Figure 5.10 shows the peaks for Er at the wavelength of 296.452 nm, wherein the analyte peak is heavily buried by both the interferent and the background matrix, resulting in Er not detectable for SARM 148 and IGS-36 samples fused in $LiBO_2$ and peroxide fusion respectively. The recovery of 236% for SARM 148 was obtained in samples digested in multi acids digestion which may be the result of the background matrix.

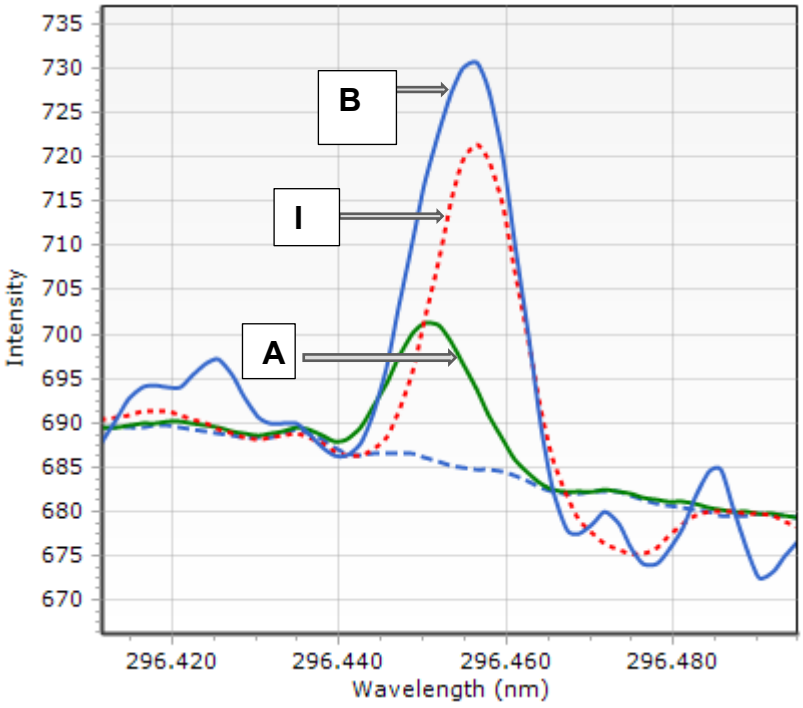

Figure 5.10 ICP-OES Spectrum for Er at wavelength (296.452nm), (A=analyte, B=Background matrix, I=interferences)

Figure 5.11 shows Gd spectrum at wavelength 301.013 nm which shows no clear peaks at the wavelength. The recoveries for both SARM 148 and IGS-36 are over 120%. The recoveries for SARM 148 are 96%, 154%, and 175% respectively while 130%, 148% obtained for IGS-36 respectively.

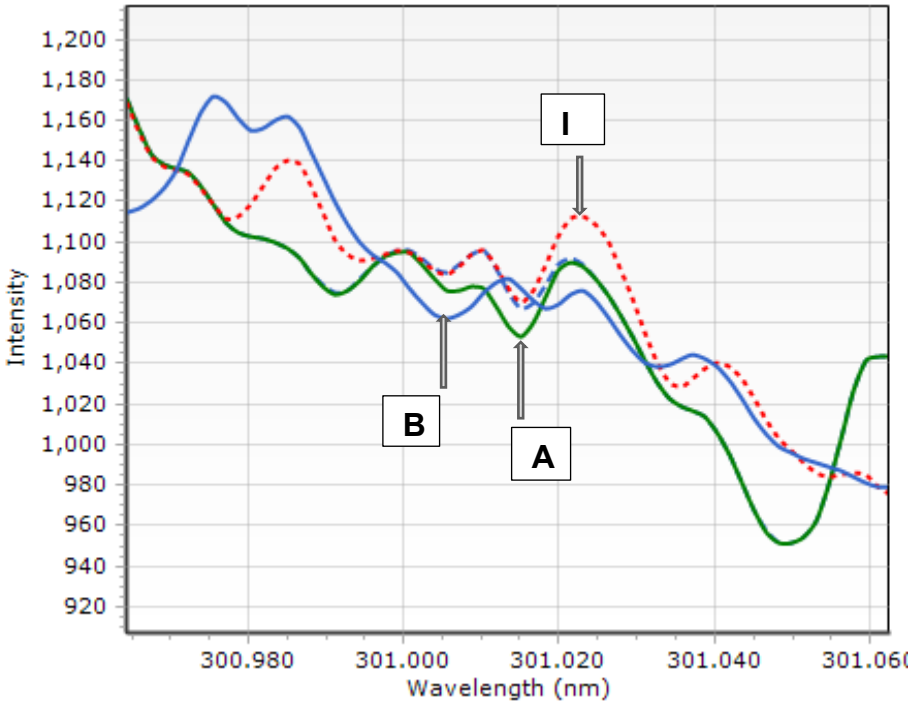

Figure 5.11 ICP-OES Spectrum for Gd at wavelength (301.013nm), (A=analyte, B=Background matrix, I=interferences)

Figure 5.12 is the spectrum for Tm at wavelength 336.261nm wherein the analyte is spectrally obscured by the interferent and the background sample matrix. The obtained recoveries for SARM 148 are 670% and 528% respectively for the peroxide and lithium metaborate fusion. The obtained recoveries for IGS-36 are 146% and 128% respectively from the samples fused by lithium metaborate and peroxide. The recovery of 118% was obtained for both the IGS-36 and SARM 148 digested using multi acids.

The observations made regarding the spectra, suggest that the increased matrix concentrations and background intensities might have directly impacted on the net intensities of the ICP-OES instrument as observed by Rucandio (1992).

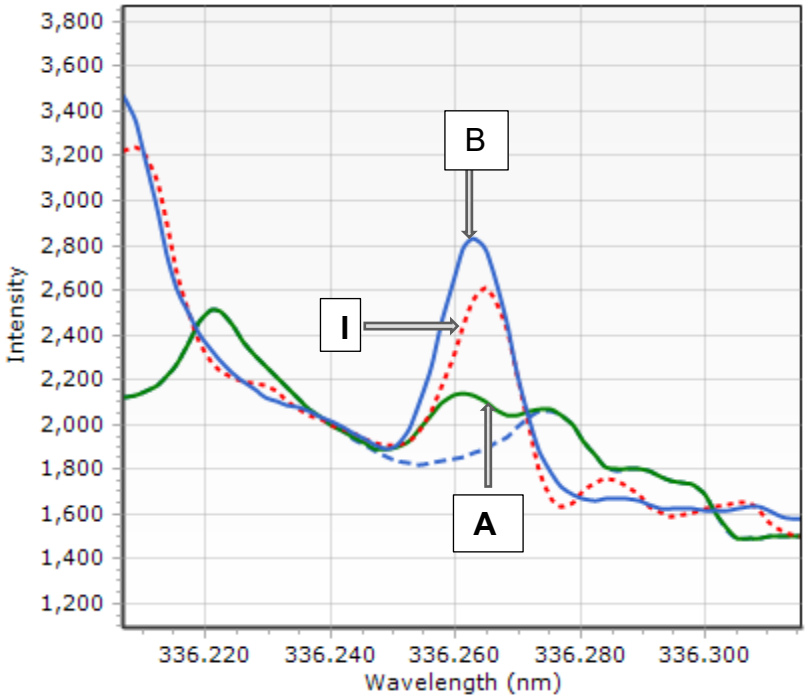

Figure 5.12 ICP-OES Spectrum for Tm at the wavelength (336.261nm), (A=analyte, B=Background matrix, I=interferences)

For all the quantified REEs using ICP-MS, the accuracy of the method as well as the recoveries ranging between 90% and 110%, have been achieved in all CRMs. The obtained data from this study was comparable with the verified values of the reference materials used. The precision measured by the RSD, most of the values achieved in this study were below 5%. Analysing various geological sample types allowed for a thorough evaluation of the established methodology's potential for quantifying REEs. According to the method description it has been demonstrated that the enhanced technique for measuring REEs in geological samples using ICP-MS is dependable and appropriate for its intended usage. The method presented analytical quality results for all the CRMs. Since there was no need for co-precipitations and /or pre-concentration steps involved, sample preparation was minimal with increased sample throughput. The alkaline fusion method ensured quick, effective, and economical dissolution method. The ICP-MS as the ultimate technique for REEs determinations revealed

excellent sensitivity, low detection limit, a broad linear range, and the precise and accurate multi-element analysis capability.

The accuracy of the method for overall recoveries ranging between 90% and 110% in all the reference materials analysed have been achieved. The obtained data from this study was comparable with the published values of the CRMs. The precision, measured by the RSD, most of the values achieved in this study were s below 8%. Using the Horwitz equation, the results obtained using different sample preparation methods is within acceptable limits of 5% variation. The results shows that the ZKD sample follows a typical cerium dominated monazite, which is the most common member, monazite-(Ce), (Ce, La, Nd, Pr, Th) PO_4, the results show yttrium (Y) concentration for ZKD to be higher than samarium (Sm) concentration, which gives this monazite a distinctive characteristic from the typical monazite- (Ce). The TREEs content for the ZKD sample is quite significant proving that South Africa have enriched reserves of critical rare earth elements such as (Dy, Sm, Tb, and Nd) required for green economy transition.

5.10 Analysis of Variance (ANOVA) for Yttrium (Y) analysis using ICP-MS

When more than two samples are compared, the analysis of variance determines whether a significant difference exists. The objective is to compare the variance and means of the various groups. ANOVA determines whether there are differences between more than two groups. As shown in figure 5.9, Yttrium quantified using ICP-MS after samples digestion using $LiBO_2$ fusion, Na_2O_2 fusion, and multi acids digestion. The average Y value of 911.9 ppm for, 1001 ppm value for Y in samples fused $LiBO_2$, and 991.6 ppm for Na_2O_2 fused samples respectively. The P-value of 0.012 is less than 0.05, null hypothesis (H_O) is rejected, and accept the alternative hypothesis (H_1) and at 95% confidence level there is minimum risk in rejecting the null

hypothesis. From this observation, statistically there is significant difference, however the values fall within the acceptable limits of the certificate of analysis for SARM 148. The significant variance may be due to fewer number of observations, or the number of replicates analysed.

Table 5.9 ANOVA results for Yttrium in SARM 148 obtained using ICP-MS

SUMMARY

Groups	*Count*	*Sum*	*Average*	*Variance*
Acid digestion	3	2735.8	911.93	129.03
$LiBO_2$ fusion	3	3003.1	1001	40.847
Na_2O_2 fusion	3	2974.7	991.58	1963.4

ANOVA

Source of Variation	*SS*	*df*	*MS*	*F*	*P-value*	*F crit*
Between Groups	14374	2	7186.9	10.107	0.012	5.1433
Within Groups	4266	6	711.08			
Total	18640	8				

CHAPTER SIX: CONCLUSION AND RECOMMENDATION

The chapter highlights the observations, failures and successes of the study. For future studies and continual improvements, recommendations are included

6.1 Conclusion

Flux fusion methods using $LiBO_2$ and Na_2O_2/NaOH as well as the hotplate assisted multi acids digestion successfully decomposed the monazite and REEs were fully liberated. Total sample dissolution was attained using the fusion methods, albeit multi acids digestion rendering partial sample dissolution, REEs were totally liberated from the sample matrix. The three dissolution methods effectively decomposed the monazite.

Employing both the ICP-OES and ICP-MS techniques for elemental analysis provided an opportunity to appreciate their differences in terms of strengths and weaknesses. The shortcomings of ICP-OES in terms of sensitivity were also observed, suggesting that separation methods for REEs from matrix elements in monazite may be necessary. The superiority and efficiency of the ICP-MS was observed, when it accurately and selectively detected rare earth elements directly in the presence of matrix elements. The light REEs such as La, Ce, Pr, Sm, Dy, as well as Y in monazite samples digested in multi acids can be accurately analysed using ICP-OES.

Sample dissolution using lithium metaborate fusion, sodium peroxide and multi acids digestion respectively are suitable methods for decomposing monazite and associated mineral for REEs determination. The flux fusion methods are easy to follow, rapid, inexpensive and ensure complete sample dissolution, while the multi acids sample digestion method lower total dissolved solids. For high sample throughput and accurate analytical result, ICP-MS finish is recommended for REEs analysis in monazite. In addition, The ANOVA results show a significant difference in Yttrium concentrations among three digestion/fusion methods for SARM 148 analysis by ICP-MS. $LiBO_2$ fusion had the highest average Yttrium concentration, followed by Na_2O_2 fusion and acid digestion. The high variance in Na_2O_2 fusion suggests inconsistency in measurements.

6.2 Recommendations

Further work is required to evaluate the matrix effect of monazite on the ICP-OES instrument sensitivity before the technique can be declared to be unfit for REE analysis in monazite. Since the ideal instrument set-up for ICP-analyses vary significantly between elements, by optimizing the system separately for each element can increase the analytical sensitivity. For evaluating the matrix impact of monazite on ICP-OES sensitivity, it is critical to optimise the instrument parameters for each rare earth element (REE). Significant results indicate that monazite introduces matrix interferences that can suppress or increase signals for specific REEs. To address this, change plasma conditions, nebuliser flow rates, and wavelengths for each REE to reduce matrix effects. In addition, matrix matching or dilution procedures might be used to eliminate interference, and alternative analytical methods such as ICP-MS or XRF could be investigated for cross-validation of ICP-OES data. The use of ICP-OES for high-precision REE analysis is promising, but it also offers hurdles due to matrix interference. To guarantee high-precision results, regular calibration checks with monazite-based standards should be included, as well as other quality control methods such as replication analyses, spike recoveries, and long-term stability testing. These steps are critical to ensuring consistent and reliable measurements. Furthermore, optimising the approach for each REE, especially those with strong matrix effects, can assist generate more consistent findings. The aforementioned recommendations are consistent with the findings, provide a road map for enhancing the application of ICP-OES in REE analysis of monazite while addressing critical issues noted by the study. To Conduct field tests to confirm the optimised ICP-OES method's resilience in real-world contexts, such as monazite mining operations.

Moreover the issues to further this research may include the comprehensive matrix studies, evaluation of alternative techniques such as

Laser Ablation ICP-MS (LA-MS), XRF which may overcome the issue of matrix interference and enhance sensitivity and accuracy.

References

Ardini, F., Soggia, F., Rugi, F., Udisti, R., & Grotti, M. (2010). Comparison of inductively coupled plasma spectrometry techniques for the direct determination of rare earth elements in digests from geological samples. *Analytica Chimica Acta*, *678*(1), 18–25. https://doi.org/10.1016/j.aca.2010.07.036

Armstrong, M. (2023). *China Dominates the Rare Earth Market*.

Balaram, V. (2019). Rare earth elements: A review of applications, occurrence, exploration, analysis, recycling, and environmental impact. *Geoscience Frontiers*, *10*(4), 1285–1303. https://doi.org/10.1016/j.gsf.2018.12.005

Balaram, V. (2023a). *Advances in Analytical Techniques and Applications in Exploration, Mining, Extraction, and Metallurgical Studies of Rare Earth Elements*. https://doi.org/10.20944/preprints202306.0479.v1

Balaram, V. (2023b). Potential Future Alternative Resources for Rare Earth Elements: Opportunities and Challenges. In *Minerals* (Vol. 13, Issue 3). MDPI. https://doi.org/10.3390/min13030425

Bezerra de Oliveira, A. L., Afonso, J. C., da Silva, L., Alcover Neto, A., Castro Carneiro, M., Dias da Silva, L. I., & Couto Monteiro, M. I. (2019). Hydrofluoric Acid-Free Digestion of Geological Samples for the Quantification of Rare Earth Elements by Inductively Coupled Plasma-Optical Emission Spectrometry. *Geostandards and Geoanalytical Research*, *43*(4), 689–699. https://doi.org/10.1111/ggr.12286

Bobba, S., Carrara, S., Huisman, J., Mathieux, F., & Pavel, C. (2020). Critical Raw Materials for Strategic Technologies and Sectors in the EU - a Foresight Study. In *European Commission*. https://doi.org/10.2873/58081

Bokhari, S. N. H., & Meisel, T. C. (2017). Method Development and

Optimisation of Sodium Peroxide Sintering for Geological Samples. *Geostandards and Geoanalytical Research*, *41*(2), 181–195. https://doi.org/10.1111/ggr.12149

Borai. EH, El-Ghany. M.S Abd, Ahmed. I.M, Hamed. M . Mostafa, Shahr El-Din. A.M, A. H. . (2016). Modified acidic leaching for selective separation of thorium, phosphate and rare earth concentrates from Egyptian crude monazite. *International Journal of Mineral Processing*, *149*, 34–41. https://doi.org/10.1016/j.minpro.2016.02.003

Chao. T.T, S. R. . (1992). Decomposition techniques. In *Journal of GeochemicalExploration* (Vol. 44).

Chao, T. T., & Sanzolone, R. F. (1992). Decomposition techniques. *Journal of Geochemical Exploration*, *44*(1–3), 65–106. https://doi.org/10.1016/0375-6742(92)90048-D

Cherviakouski, K., Pandey, O. P., Liu, J., & van der Zwan, F. M. (2024). Application of microwave digestion for complete dissolution of igneous silicate rock samples: A simple and quick sample preparation procedure. *Talanta*, *277*(June), 126377. https://doi.org/10.1016/j.talanta.2024.126377

Chi. R, W. D. (1996). Rare earth ore processing and extraction technology. *Science Publishing Company*, *293*, 305–332.

Cotta, A. J. B., & Enzweiler, J. (2012). Classical and New Procedures of Whole Rock Dissolution for Trace Element Determination by ICP-MS. *Geostandards and Geoanalytical Research*, *36*(1), 27–50. https://doi.org/10.1111/j.1751-908X.2011.00115.x

Cotton.S. (2006). *Lanthanide and Actinide Chemistry*. John Wiley and Sons.

Eggins .S.M, Woodhead J.D, Kingsley. L.P.J, Mortimer. G.E, Sylvester. P, McCulloch . M.T, Hergt .J.M, H. M. . (1997). n ! Zi-internal standardisation. *Chemical Geology*, *1*(134), 311–326.

Ferron, C.J., Bulatovic, S.M., Salter, R. . (1991). Beneficiation of

Rare Earth Oxide Minerals. *Materials Science ForumMaterials Science Forum*, *70*(72), 251–270. https://doi.org/https://doi.org/10.4028/www.scientific.net/msf.70-72.251.

Filho. Walter Leal, Kotter. Richard, Özuyar. Pinar Gökçin, Abubakar. Ismaila .Rimi, Eustachio. João. Henrique Paulino. Pires, M. N. R. (2023). Understanding Rare Earth Elements as Critical Raw Materials. *Sustainability (Switzerland)*, *15*(3). https://doi.org/10.3390/su15031919

Greinacher, E. (1981). History of Rare Earth Applications, Rare Earth Market Today. *ACS Publication*, 3–17.

Greinacher, E. (2024). *Downloaded via 41.13.104.230 on October 30* (Vol. 19). UTC.

Gupta .Chiranjib.Kumar, K. N. (2015). *Extractive metallurgy of rare earths, second edition* (second). CRC Press. https://doi.org/https://doi.org/10.1201/b19055

Gupta, C. K. ., & Krishnamurthy, N. . (2005). *Extractive metallurgy of rare earths*. CRC Press.

Haque, N., Hughes, A., Lim, S., & Vernon, C. (2014). *Rare Earth Elements: Overview of Mining, Mineralogy, Uses, Sustainability and Environmental Impact*. 614–635. https://doi.org/10.3390/resources3040614

Helmeczi, E., Wang, Y., & Brindle, I. D. (2016). A novel methodology for rapid digestion of rare earth element ores and determination by microwave plasma-atomic emission spectrometry and dynamic reaction cell-inductively coupled plasma-mass spectrometry. *Talanta*, *160*, 521–527. https://doi.org/10.1016/j.talanta.2016.07.067

Hu, Z., & Qi, L. (2014). Sample Digestion Methods. In *Treatise on Geochemistry: Second Edition* (Vol. 15, pp. 87–109). Elsevier Inc. https://doi.org/10.1016/B978-0-08-095975-7.01406-6

Jarvis, I., & Jarvis, K. E. (1992a). Plasma spectrometry in the earth

sciences: techniques, applications and future trends. In *Chemical Geology* (Vol. 95).

Jarvis, I., & Jarvis, K. E. (1992b). Plasma spectrometry in the earth sciences: techniques, applications and future trends. *Chemical Geology*, *95*(1–2), 1–33. https://doi.org/10.1016/0009-2541(92)90041-3

Jepson, N. (2012). *A 21stcentury scramble: South Africa, China and the rare earth metals industry*.

Jowitt, S. M. (2022). Mineral economics of the rare-earth elements. *MRS Bulletin*, *47*(3), 276–282. https://doi.org/10.1557/s43577-022-00289-3

Kumari, A., Panda, R., Jha, M. K., Kumar, J. R., & Lee, J. Y. (2015). Process development to recover rare earth metals from monazite mineral: A review. In *Minerals Engineering* (Vol. 79, pp. 102–115). Elsevier Ltd. https://doi.org/10.1016/j.mineng.2015.05.003

Kumari, A., Panda, R., Kumar, M., Kumar, J. R., & Young, J. (2015). Process development to recover rare earth metals from monazite mineral : A review. *Minerals Engineering*, *79*, 102–115. https://doi.org/10.1016/j.mineng.2015.05.003

Longerich H.P, Jenner G.A, Fryer B.J, J. S. . (1990). Inductively coupled plasma-mass spectrometric analysis of geological samples: A critical evaluation based on case studies. *Chemical Geology*, *83*(1–2), 105–118. https://doi.org/https://doi.org/10.1016/0009-2541(90)90143-U

Makombe, M., Horst, C. van der, Silwana, B., Iwuoha, E., & Somerset, V. (2017). Optimisation of Parameters for Spectroscopic Analysis of Rare Earth Elements in Sediment Samples. In *Rare Earth Element*. InTech. https://doi.org/10.5772/intechopen.68280

Matusiewicz, H. (2003). Wet digestion methods. *Comprehensive Analytical Chemistry*, *43*(2003), 193–233.

https://doi.org/https://doi.org/10.1016/S0166-526X(03)41006-4

Mnculwane, H. T. (2022a). Rare Earth Elements Determination by Inductively Coupled Plasma Mass Spectrometry after Alkaline Fusion Preparation. *Analytica*, *3*(1), 135–143. https://doi.org/https://doi.org/10.3390/analytica3010010

Mnculwane, H. T. (2022b). Rare Earth Elements Determination by Inductively Coupled Plasma Mass Spectrometry after Alkaline Fusion Preparation. *Analytica*, *3*(1), 135–143. https://doi.org/10.3390/analytica3010010

Mohammed A. Alam, Leonard Zuga, M. G. P. (2012). Economics of rare earth elements in ceramic capacitors. *Ceramics International*, *38*(8), 6091–6098. https://doi.org/http://dx.doi.org/10.1016/j.ceramint.2012.05.068

Moila. Awelani Veronica. (2019). *Process Mineralogy and Extraction of Rare Earth Elements from Beach Placer Deposit* (Issue February). University of Witwatersrand.

Morrison, W. M., & Tang, R. (2012). China's rare earth industry and export regime: Economic and trade implications for the United States. *Rare Earth Elements: Supply, Trade and Use Dynamics*, 27–63.

Murty. D.S R, Balaji. B.K, B. S. . (1990). *summary-2024-09-13T07_35_57Z*. *11*, 112–115.

Orris, G. J., & Grauch, R. I. (2002). Rare earth element mines, deposits, and occurrences. *Open-File Report 02-189*, *January 2002*, 174.

Padmasubashini. Veeraraghavan, Sunilkmar. Beena, Krishnakumar. M, S. S. B. (2020). Masubashini et al 2020. *Chemical Geology*, *6*(3), 98–109.

Padmasubashini, V. (2022). Method validation and uncertainty for the determination of rare earth elements, yttrium, thorium and

phosphorus in monazite samples by ICP-OES. *Chemistry International*, *6*(3), 98–109.

Padmasubashini, V., Sunilkumar, B., Krishnakumar, M., & Singh, S. B. (2022). *Method validation and uncertainty for the determination of rare earth elements , yttrium , thorium and phosphorus in monazite samples by ICP-OES Method validation and uncertainty for the determination of rare earth elements , yttrium , thorium and phospho*. *May*.

Padmasubashinia, V., & Satyanarayana, K. (2013). Determination of rare earth elements, yttrium, thorium, and other trace elements in monazite samples by inductively coupled plasma mass spectrometry. *Atomic Spectroscopy*, *34*(1), 6–14. https://doi.org/10.46770/as.2013.01.002

Panteeva, S. V., Gladkochoub, D. P., Donskaya, T. V., Markova, V. V., & Sandimirova, G. P. (2003). Determination of 24 trace elements in felsic rocks by inductively coupled plasma mass spectrometry after lithium metaborate fusion. *Spectrochimica Acta - Part B Atomic Spectroscopy*, *58*(2), 341–350. https://doi.org/10.1016/S0584-8547(02)00151-9

Parthasarathy. P, Desai. H.B, K. S. . (1986). Radiochemical neutron activation analysis of individual rare earth elements in monazites from different geological environments. *J. Radioanal. Nucl. Chem.*, *105*(5), 277–290.

Potts , P, J, R. P. (2003). Sample preparation of geological samples, soils and sediments. *Comprehensive Analytical Chemistry*, *41*, 723–763. https://doi.org/https://doi.org/10.1016/S0166-526-x(03)41024-6

Premadas. A, K. C. . (2006). Solvent extraction separation of heavy rare earth elements from light rare earth elements and thorium. *Atomic Spectroscopy*, *27*(5), 170–177.

Premadas, * A, & Khorge, C. R. (2006). Solvent Extraction Separation of Heavy Rare Earth Elements From Light Rare

Earth Elements and Thorium: ICP-AES Determination of REEs and Yttrium in Monazite Mineral. In *Atomic Spectroscopy* (Vol. 27, Issue 5).

Premadas, A., & Khorge, C. R. (2006). Solvent extraction separation of heavy rare earth elements from light rare earth elements and thorium: ICP-AES determination of REEs and yttrium in monazite mineral. *Atomic Spectroscopy*, *27*(5), 170–177.

Radhamani, R., Murugesan, P., & Srivastava, P. K. (2007). Rapid decomposition of monazite and xenotime for determination of Th and REE by inductively coupled plasma emission spectrometry. *Exploration and Research for Atomic Minerals*, *17*, 174–179.

Rucandio, M. I. (1992). Determination of lanthanides and yttrium in rare earth ores and concentrates by inductively coupled plasma atomic emission spectrometry. *Anal. Chim. Acta*, *264*(2), 333–344. https://doi.org/https://doi.org/10.1016/0003-2670(92)87023-E

Sappin, A.-A., & Beaudoin, G. (2015). *Rare earth elements in Québec, Canada: Main deposit types and their economic potential*.

Saputra H.Anggraeni Mutalib A, B. (2021). Development of a Fast Simultaneous Analysis Method for Determination of Middle Rare-Earth Elements in Monazite Samples. *Jurnal Kimia Sains Dan Aplikasi*, *24*(5), 177–184. https://doi.org/https://doi.org/10.14710/jksa.24.5.177-184

Scherrer, N. C., Engi, M., Gnos, E., Jakob, V., & Liechti, A. (2000). *Monazite analysis ; from sample preparation to microprobe age dating and REE quantification*. 93–105.

SEELYE, F. T., & RAFTER, T. A. (1950). Low-Temperature Decomposition of Rocks, Ores and Minerals by Sodium Peroxide using Platinum Vessels. *Nature*, *165*(4191), 317.

https://doi.org/10.1038/165317a0

Sen Gupta. J.G, B. N. . (1995). Direct ICP-MS determination of trace and ultratrace elements in geological materials after decomposition in a microwave oven. Part II. Quantitation of Ba, Cs, Ga, Hf, In, Mo, Nb, Pb, Rb, Sn, Sr, Ta and Tl. *Talanta*, *42*(12), 1947–1957. https://doi.org/10.1016/0039-9140(95)01673-2

Sen Gupta, J. G., & Bertrand, N. B. (1995). Talanta Direct ICP-MS determination of trace and ultratrace elements in geological materials after decomposition in a microwave oven I. Quantitation of Y, Th, U and the lanthanides. In *Talanta* (Vol. 42).

Seredin, V.V and Dai, S. (2012). Coal deposits as potential alternative sources for lanthanides and yttrium. *International Journal of Coal Geology*, *94*(2012), 67–93. https://doi.org/:10.1016/j.coal.2011.11.001

Syed, Hussain, N., & Ph, B. (2016). *D evelopment of Measurement procdure for rapid analysis of Major, Rare Earth and platinum group elements in geological*. *August*.

Taicheng D., H. C. and X. Z. (2002). Determination of rare and rare earth elements in soils and sediments by ICP -MS using Ti(OH) 4 –Fe(OH) 3 co -precipitation preconcentration. *Journal of Analytical Atomic Spectrometry*, *17*, 410 –413.

Walters Abigail, L. P. (2011). *Rare earth elements*.

Xaba. SM, Nete. M, P. W. (2018). Concentration of rare earth elements from monazite by selective precipitation. *Concentration of Rare Earth Elements from Monazite by Selective Precipitation*, 1–7. https://doi.org/10.1088/1757-899X/430/1/012006

Xaba, Nete, M., & Purcell, W. (2018a). Concentration of rare earth elements from monazite by selective precipitation. *IOP Conference Series: Materials Science and Engineering*,

430(1). https://doi.org/10.1088/1757-899X/430/1/012006

Xaba, S., Nete, M., & Purcell, W. (2018b). Concentration of rare earth elements from monazite by selective precipitation. *IOP Conference Series: Materials Science and Engineering*, 1–7.

Yadav, A., Bhowmik, D., & Sikder, N. (2012). Direct determination of zirconium and silicon in zircon by flame atomic absorption spectrometry using two rapid decomposition methods. *Analytical Methods*, *4*(8), 2454–2461. https://doi.org/10.1039/c2ay25177a

Yokoyama. T, Makishima. A, N. E. (1999). Evaluation of the coprecipitation of incompatible trace elements with fluoride during silicate rock dissolution by acid digestion. *Chemical Geology*, *157*(3–4), 175–187. https://doi.org/https://doi.org/10.1016/15009-2541(98)00206-x

Zaman, M. M. (. (2015). *Crystal Chemistry of Zircon and Monazite: Crystal Structure, Major and Trace Elements, and Radiation Damage* [University of Calgary, Calgary, Canada]. https://doi.org/https://prism.ucalgary.ca. doi:10.11575/PRISM/25497

Zhang, W., & Hu, Z. (2019). Spectrochimica Acta Part B Recent advances in sample preparation methods for elemental and isotopic analysis of geological samples. *Spectrochimica Acta Part B*, *160*(August), 105690. https://doi.org/10.1016/j.sab.2019.105690

Zhang, W., Hu, Z., Liu, Y., Chen, H., Gao, S., & Gaschnig, R. M. (2012). Total rock dissolution using ammonium bifluoride (NH4HF 2) in screw-top Teflon vials: A new development in open-vessel digestion. *Analytical Chemistry*, *84*(24), 10686–10693. https://doi.org/10.1021/ac302327g

Zhang, W., Hu, Z., Liu, Y., Chen, L., Chen, H., Li, M., Zhao, L., Hu, S., & Gao, S. (2012). Reassessment of HF/HNO 3 Decomposition Capability in the High-Pressure Digestion of

Felsic Rocks for Multi-Element Determination by ICP-MS. *Geostandards and Geoanalytical Research*, *36*(3), 271–289. https://doi.org/10.1111/j.1751-908X.2012.00156.x

Zuma. Mceliseni. C, L. (2022). Recent trends in sample preparation methods and plasma-based spectrometric techniques for the determination of rare earth elements in geological and fossil fuel samples. *Applied Spectroscopy Reviews*, *57*(5), 353–377. https://doi.org/10.1080/05704928.2020.1858093

Appendix 1

The table of selected wavelengths and isotopes.

Element	**Selected isotopes in ICP-MS analysis**	**Selected wavelengths in ICP-OES analysis (nm)**
Y	89	224.303 and 324.228
La	139	492.178 and 398.852
Ce	140	456.236, 418.659 and 447.124
Pr	141	406.281 and 411.846
Nd	146	380.533 and 397.326
Sm	147	388.528 and 388.528
Eu	153	412.972, 272.778 and 281.393
Gd	157	310.050 and 301.013
Tb	159	370.392 and 332.440
Dy	163	353.171 and 400.045
Ho	165	345.600 and 339.895
Er	166	296.452 and 326.478
Yb	172	222.447, 212.674 and 224.303
Tm	169	336.261 and 384.802
Lu	175	296.332, 219.556 and 296.332

Re	187	202.364, 221.427 and 227.525
In	115	230.606, 303.936 and 325.609

Appendix 2

Certified values for SARM148

13. PROPERTY VALUES

Property values

Certified	Unit	Average	Lab S	N
Ce	ppm	22742	1770	7
Certified	Unit	Average	Lab S	N
La	ppm	11975	458	7
Certified	Unit	Average	Lab S	N
Nd	ppm	9462	452	8
Certified	Unit	Average	Lab S	N
Pr	ppm	2633	167	7
Certified	Unit	Average	Lab S	N
Sm	ppm	1494	134	8
Certified	Unit	Average	Lab S	N
Dy	ppm	282	30.5	8
Certified	Unit	Average	Lab S	N
Eu	ppm	33.1	4.37	7
Certified	Unit	Average	Lab S	N
Gd	ppm	840	45.2	8
Certified	Unit	Average	Lab S	N
Ho	ppm	39.2	3.60	7
Certified	Unit	Average	Lab S	N
Er	ppm	96.9	16.9	7
Certified	Unit	Average	Lab S	N
Tb	ppm	93.4	15.6	7
Certified	Unit	Average	Lab S	N
Tm	ppm	7.76	1.729	7
Certified	Unit	Average	Lab S	N
Yb	ppm	51.4	4.81	7
Certified	Unit	Average	Lab S	N
Lu	ppm	7.18	0.796	7
Certified	Unit	Average	Lab S	N
Y	ppm	969	139	8
Certified	Unit	Average	Lab S	N
U	ppm	338.45	34.047	7
Certified	Unit	Average	Lab S	N
Th	ppm	8844	823	6

Appendix 3

CERTIFICATE OF ANALYSIS

SARM 148
Monazite ore

1. **STATUS OF CERTIFICATE**

   This is the first issue of the certificate.

2. **DATE OF ORIGINAL CERTIFICATION**

   2015-11-30

3. **AVAILABILITY OF THE MATERIAL**

   100 g units of the pulverised material are available.

4. **SOURCE AND SUPPLIER OF THE MATERIAL**

   The material was supplied by Mineral Processing Division of MINTEK, sourced from Richards bay Minerals, South Africa.

5. **PREPARER OF THE REFERENCE MATERIAL**

   The reference material was prepared by Mintek's Analytical Services Division

6. **DESCRIPTION OF THE MATERIAL**

   Monazite ore, characterised by the mineralogical composition, tabulated below.

Table1: Relative abundance of minerals compositions of SARM 148 material

Mineral	Ideal Chemical Formula	Relative Abundance	Mass (%)
Ilmenite	$FeTiO_3$	major	25 - 50
Monazite	$(Ce,La,Nd,Th)PO_4$	intermediate	15 - 25
Hematite	Fe_2O_3	minor	5 - 15
Rutile	TiO_2	minor	5 - 15
Quartz	SiO_2	intermediate	15 - 25
Zircon	$ZrSiO_4$	minor	5 - 15

Certificate of analysis for SARM 148

Appendix 4

Spectrums for ICP-OES showing direct overlap and wing overlap of emission lines of interfering elements on the analyte

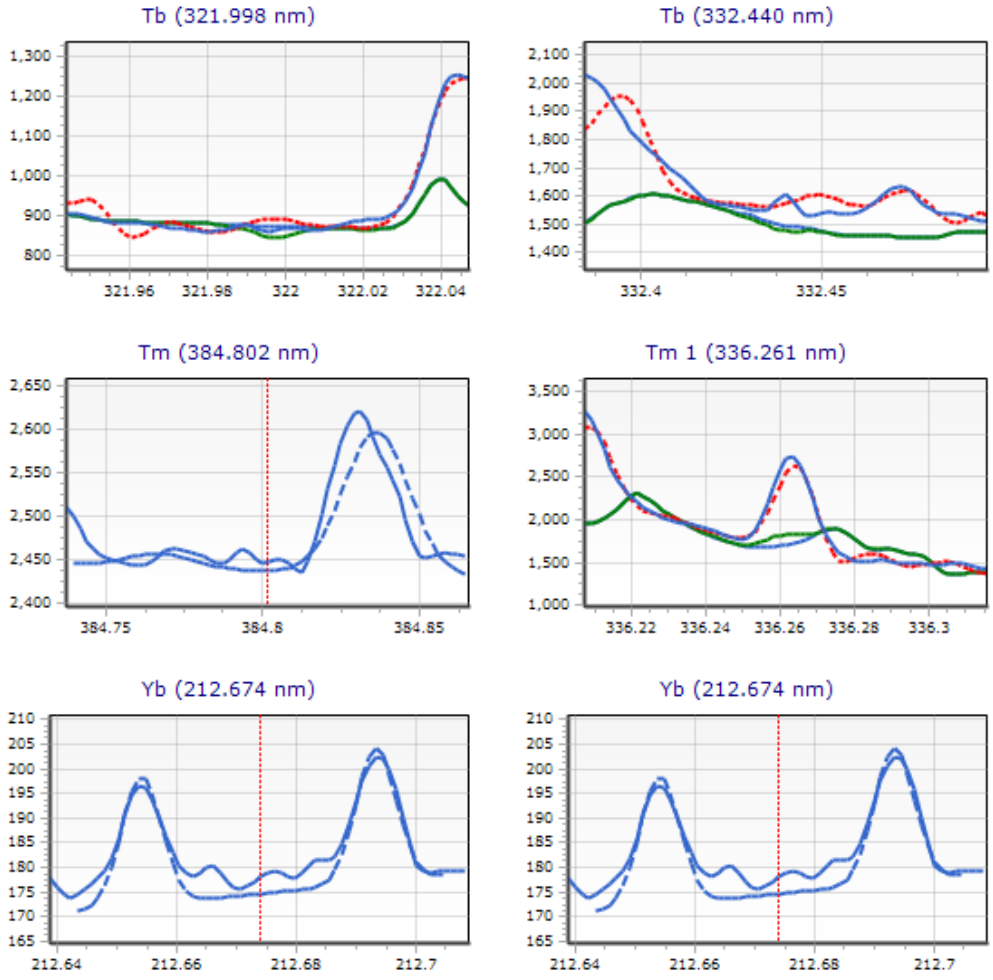
Tb (321.998 nm)
Tb (332.440 nm)
Tm (384.802 nm)
Tm 1 (336.261 nm)
Yb (212.674 nm)
Yb (212.674 nm)

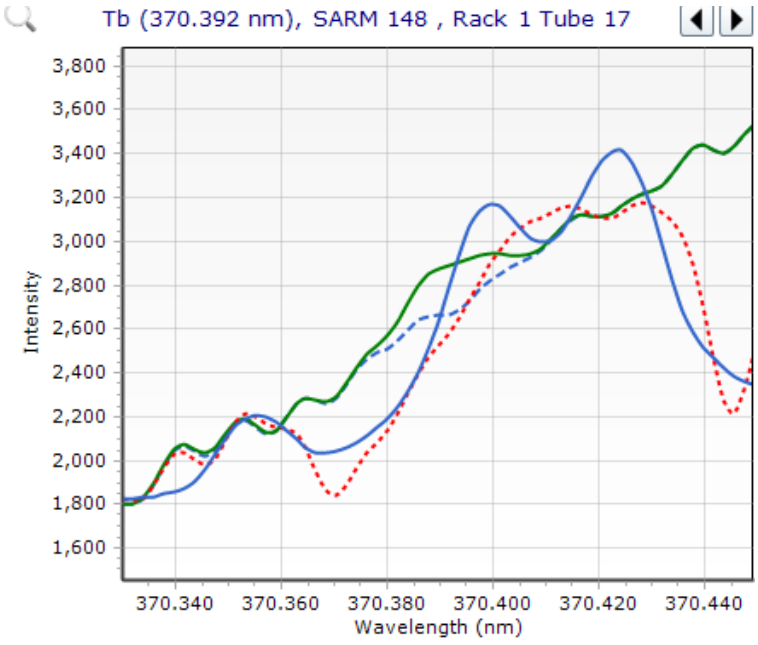
Tb (370.392 nm), SARM 148 , Rack 1 Tube 17
Intensity
Wavelength (nm)